Scuola Internazionale Superiore Studi Avanzati-S.I.S.S.A-
International School for Advanced Studies -I.S.A.S-

Trieste, Italy


# Promotion of embryonic cortico-cerebral neuronogenesis by miR-124

Thesis submitted for the degree of "Doctor Philosophiae"

Academic Year 2008/2009

Candidate
Maiorano Nicola Antonio

Supervisor
Prof Antonello Mallamaci

# Promotion of embryonic cortico-cerebral neuronogenesis by miR-124

Candidate
Maiorano Nicola Antonio

Supervisor
Prof Antonello Mallamaci

# Index

*To Germano*

# Abstract

Glutamatergic neurons of the murine cerebral cortex are generated within periventricular proliferative layers of the embryonic pallium, directly from apical precursors or indirectly, via their basal progenies. Cortical neuronogenesis is the result of different morphogenetic subroutines, including precursors proliferation, death, changes of histogenetic potencies, post-mitotic neuronal differentiation. Control of these processes is extremely complex and numerous polypeptide-encoding genes are involved in it. Moreover, a large number of so-called "non-coding genes" are expressed in the developing cortex too. At the moment, their implication in corticogenesis is subject of intensive functional studies. A subset of them encodes for miRNAs, a class of small RNAs with complex biogenesis, regulating gene expression at multiple levels, modulating histogenetic progression and implicated in refinement of positional information. Among cortical miRNAs, there is miR-124. It has been consistently shown to promote neuronogenesis progression, in a variety of experimental contexts. Some aspects of its activity - however - are still controversial, some have to be clarified. An in depth *in vivo* characterization of its function in the embryonic mammalian cortex is still missing.

In this study, by integrating LNA-oligo *in situ* hybridization, electroporation of stage-specific reporters and immunofluorescence, we reconstructed the cortico-cerebral miR-124 expression pattern, during direct neuronogenesis from apical precursors and indirect neuronogenesis, via basal progenitors. We found that miR-124 expression profile in the developing embryonic cortex includes an abrupt upregulation in apical precursors undergoing direct neuronogenesis as well as a two-steps upregulation in basal progenitors, during indirect neuronogenesis. Differential post-transcriptional processing seems to contribute to this pattern. Moreover, we investigated the role of miR-124 in embryonic corticogenesis by gain-of-function approaches, both *in vitro,* by lentivirus-based gene transfer, and *in vivo*, by *in utero* electroporation. Following overexpression of miR-124, both direct neuronogenesis and progression of neural precursors from the apical to the basal compartment were stimulated.

Two are the main conclusions of this study. First, miR-124 expression is progressively up-regulated in the mouse embryonic neocortex, during the apical to basal transition of neural precursor cells and upon their exit from cell cycle. Second, miR-124 is involved in fine regulation of these processes.

# 1. Introduction

## 1.1 Generalities on cerebral cortex morphogenesis: definition of the cortical field and histological maturation of the cortical primordium

In mice, from embryonic day 7.5 (E7.5), the Central Nervous System (CNS) is derived from the neural plate, a region of dorsal ectoderm with a columnar cellular phenotype which, after gastrulation, thickens and rises at its borders, invaginates in neural groove and closes dorsally to form a hollow cylinder, the neural tube (Gilbert 7th edition, 2003). Cells at the interface between the dorsal neural tube and the overlying epithelium are called neural crest cells (NCSs). Such cells acquire a migratory behavior and are bound to give rise to peripheral nervous system (PNS) melanoctyes, and head skeletal elements (Liu and Niswander 2005) (fig. 1A). At this stage the anterior neural plate gives rise to the prosencephalon, a vesicle which is subsequently subdivided into the telencephalon and the diencephalon (fig. 1B). After the initial induction of neural tissue, the cortical primordium is formed at the rostral most portion of the neural tube and is quickly subdivided into two halves: the left and right telencephalic vesicles (the future cerebral hemispheres). In particular, at embryonic day 8 (E8.0, four to eight somites), the mouse telencephalic anlage lies within the anterior third of the paired, downward-folded leaves of the neural plate, and the two sides of the anlage meet at the anterior midline. By coupling a dramatic set of morphogenetic movements with extensive proliferation, the telencephalon is transformed, by around embryonic day 9.5 (E9.5, the 20-somite stage), into a set of paired vesicles, complete with regionally restricted markers (fig.1C). The subdivision into two halves -the left and right telencephalic vesicles- depends on the dorsal midline roof plate, where low levels of proliferation and high levels of apoptosis result in its fixation and invagination relative to the rapidly expanding hemispheres (Monuki and Walsh, 2001). As these events proceed, the cortical primordium field is progressively specified being exposed to several potential sources of secreted signaling molecules from surrounding structures, often called ‘organizers’, such as the anterior neural ridge (ANR) in the rostral midline, the roof plate (RF) and the cortical hem at the dorsal midline and other potential sources of signaling molecules, such as the surface ectoderm (the future skin) and mesenchymal elements that lie between the skin and brain (fig.1D). Such signaling molecules together with transcription factor genes expressed by the field itself regulate both the anterior-posterior (AP) and the dorsal-ventral (DV) patterning of neural tissue (Wilson and Rubenstein, 2000; Mallamaci and Stoykova, 2006). In the telencephalic anlage the presence of transcription factors and regionally restricted markers are a presage to the morphological

appearance of discrete dorsal (cortex), lateral (lateral ganglionic eminence or LGE) and ventral (medial ganglionic eminence or MGE) proliferative zones, around embryonic day 11.5 (E11.5) (Rallu et al., 2002).

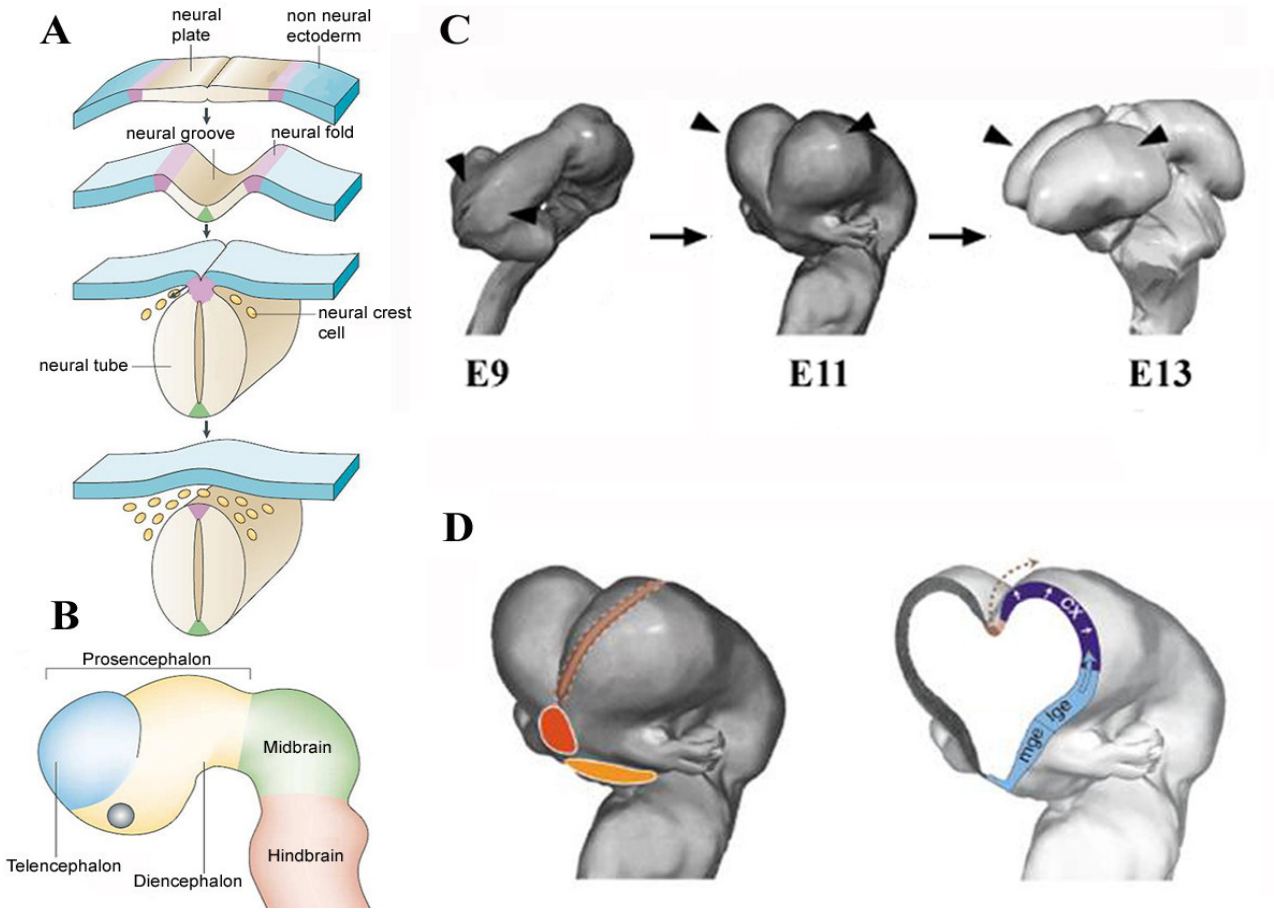


**Figure 1. Morphogenesis of the forebrain.** **(A)** The CNS arises from a specialized epithelium, the neural plate. At the end of neurulation the lateral edges of the neural plate fuse and segregate from the non-neural epithelium to form a neural tube. **(B)** The anterior neural tube gives rise to the prosencephalon, a vesicle which is subsequently subdivided into the telencephalon and the diencephalon. **(C)** Schematic three-dimensional view of forebrain morphogenesis from the time of rostral neural tube closure (E9 in mice) through the formation of the two telencephalic (cerebral) vesicles (E11 in mice). At the time of neural tube closure, the telencephalic vesicles (cerebral hemispheres) are not morphologically detectable. **(D)** Schematic of the E11 rat forebrain, illustrating the locations of the organizer centers prechordal mesoderm (orange), anterior neural ridge (red), roof plate and cortical hem (brown). Each of these organizers is associated with a particular growth factor or family of factors. Coronal view of the E11 mouse forebrain illustrate the dorsal (cortex), lateral (LGE) and ventral (MGE) proliferative zones. Arrowheads indicate location of telencephalic vesicles. Adapted from Monuki and Walsh (2001); Liu and Niswander (2005).

The cortical primordium of the E11.5 mouse embryo, looks like a thin neuroepithelial sheet and does not display any major region-specific morphological peculiarity. Subsequently it undertakes a complex and articulated process of regional diversification leading to the development of the mature cerebral cortex with its full repertoire of area-specific properties.

## 1.2 Area and laminar differentiation of the cortical primordium

In mice the cortical primordium, from E11.5 to E17.5, is subject to a dramatic expansion. Such process will give rise to the neuronal complement of the mouse cerebral cortex, which is divided into distinct zones differing in terms of cell type and arrangement, projection targets and molecular markers (fig. 2) (Molyneaux et al., 2007). The neocortex is the largest region; it is organized in six radial layers and is positioned between two other regions of the cerebral cortex, the archicortex (including entorhinal cortex, retrosplenial, subiculum, and hippocampus) and paleocortex (olfactory piriform cortex) which are organized in three radial layers (fig.2) (O'Leary et al., 2007). Each layer of the neocortex, which can be substratified, contains a population of neurons that is morphologically, connectionally, and functionally distinct from those of other layers. In its tangential dimension, the neocortex is organized into ''areas'' (fig.2); these are functionally unique subdivisions distinguished from one another by differences in cytoarchitecture and chemoarchitecture, input and output connections, and patterns of gene expression. Intrinsic genetic effectors such as transcription factors (TFs) have been demonstrated to have a role in specifying the tangential, positional identities of cortical progenitors (Bishop et al., 2000; Mallamaci et al., 2000). However extrinsic agents such as talamocortical axon (TCA) inputs have an important role for the area patterning (O'Leary and Nakagawa 2002).

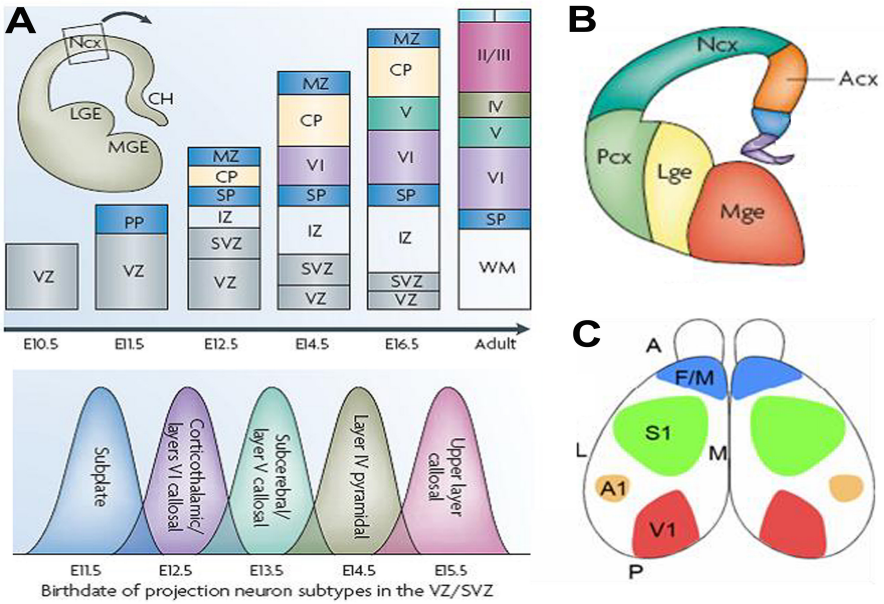


**Figure 2. Specification of neocortical progenitors in layers and areas. (A)** Neural progenitors residing in the VZ and SVZ in mice produce projection neurons in an 'inside-out' fashion. **(B)** Specification during differentiation of telencephalic areas (Ncx, neocortex; Lge, lateral ganglionic eminence; Mge, medial ganglionic eminence; Pcx, paleocortex; Acx, paleocortex). **(C)** Differentiation of Neocortical progenitors gives rise to the anatomically and functionally distinct areas seen in the adult (F/M motor cortex; S sensorial cortex; V visual cortex; A auditory cortex). Adapted from Molyneaux et al. (2007) and O'Leary et al. (2007).

In the cortical primordium neural progenitors are generated adjacent to the lateral ventricles, within the so-called ventricular zone (VZ). As neurogenesis proceeds, an additional proliferative layer known as the subventricular zone (SVZ) forms above the VZ (Bayer and Altman, 1991). Newborn neurons can move to their final destination following a radial direction and settling at distinctive radial levels, depending on their birthdates (Nadarajah and Parnavelas, 2002). Progenitors residing in the VZ and SVZ produce the projection neurons of the different neocortical layers in a tightly controlled temporal way (fig.2). The earliest born neurons appear around E10.5 in the mouse and form a layered structure termed the preplate (PP), which is later split into the more superficial marginal zone (MZ) and the deeply located subplate (SP). The cortical plate begins to develop in between these two layers, such that later born neurons arriving at the cortical plate migrate past earlier born neurons. Different classes of projection neuron are born in overlapping temporal waves (Molyneaux et al., 2007). Early cortical progenitors, normally fated to form deep layer neurons, are multipotent and can generate later born neurons of upper layers in appropriate condition (McConnell and Kaznowski, 1991). On the other side progenitors of the upper layers have less plasticity (Frantz and McConnell, 1996).

### 1.3 Origin of glutamatergic vs. gabaergic neurons

The radial migration route is typically undertaken by the future projection neurons, a large population of excitatory glutamatergic cortical neurons (fig.3) (Rash and Grove, 2006). Such neurons are characterized by a typical pyramidal morphology and transmit information between different regions of the neocortex and to other regions of the brain (Molyneaux et al., 2007). However, newborn neurons can also follow a tangential migration route reaching a final destination that can be very distant from their birth place (Marin and Rubenstein, 2001). The cortical interneurons, which account for about 20% of all cortical neurons, are Gabaergic and also typically express distinct neuropeptides that define subclasses of it (Cherubini and Conti, 2001; Wonders and Anderson, 2006). In mice, from E12 to E15, they are generated primarily from progenitors within ventral telencephalon, earlier in the MGE and the caudal ganglionic eminences (CGE), later in the LGE, and migrate along multiple pathways to reach the cortex (fig.3) (Marin and Rubenstein, 2003). Once within the cortex, they migrate along tangentially aligned pathways in the MZ and intermediate zone (IZ), and eventually turn and migrate radially into the cortical plate (CP), perpendicular to their original tangential path (Nadarajah and Parnavelas, 2002). A third, but proportionally very small general category of cortical neurons, are Cajal-Retzius neurons, which populate the MZ and express Reelin, a large secreted protein thought to be required to establish appropriate cortical layering by influencing the radial

migration and the patterning of cortical neurons (Feng and Walsh, 2001; Tissir and Goffinet, 2003). Cajal-Retzius neurons are also generated external to the cortical VZ and SVZ, primarily within the cortical hem but additionally at other sites in the subpallium and septum (fig.3) (Yamazaki et al., 2004; Bielle et al., 2005; Guillemot, 2005). In this way multiple progenitor zones contribute to the rich variety of neuronal types found in the neocortex.

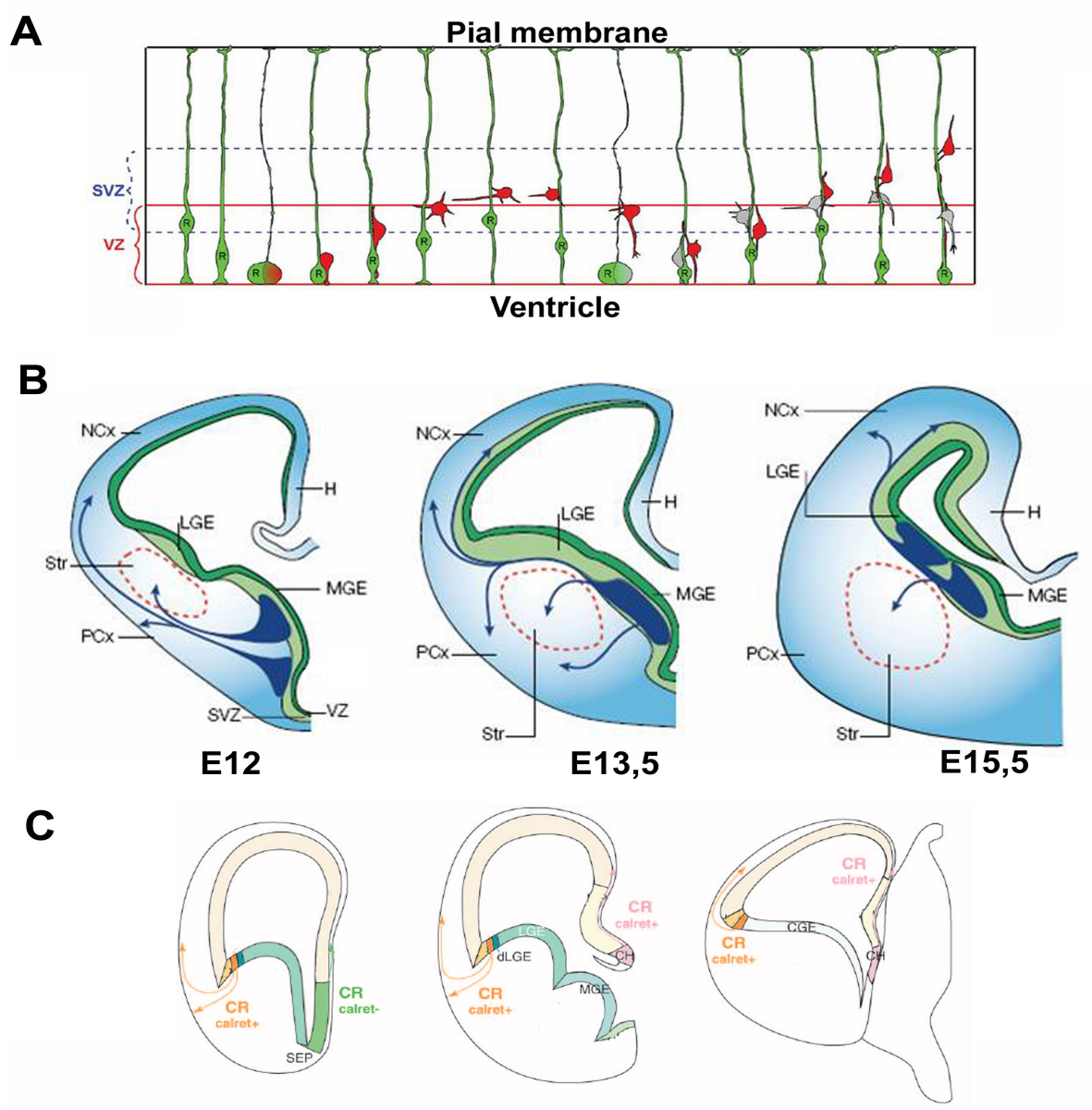


**Figure 3. Main neuronal migrations during the development of forebrain in mouse. (A)** Radial migration of differentiating neurons from the proliferative layers of cortical primordium towards the layers of the neocortex below the pial membrane. **(B)** Routes of tangential migration of immature interneurons from the subpallial telencephalon to the cortex at E12, E13.5 and E15 (NCx neocortex; H, hippocampus; PCx, piriform cortex; VZ, ventricular zone; SVZ, subventricular zone; MGE, medial ganglionic eminence; LGE, lateral ganglionic eminence; Str, striatum). **(C)** Distinct populations of Cajal–Retzius cells (CR; calret+ denotes the presence of calretinin) have been shown to originate from cortical hem (CH), septum (SEP), pallial-subbpallial boundary (PSPB)**.**. Adapted from Noctor et al. (2004), Marin and Rubenstein (2001), Guillemot (2005).

## 1.4 Neocortical periventricular proliferative layers: apical and basal compartments

During all neurogenesis, within the developing neocortex, there are at least three different types of neurogenic progenitors: neuroepithelial progenitor cells (NEPs), radial glia cells (RGCs) and intermediate progenitors cells (IPCs) (Gotz and Huttner, 2005) (fig.4).

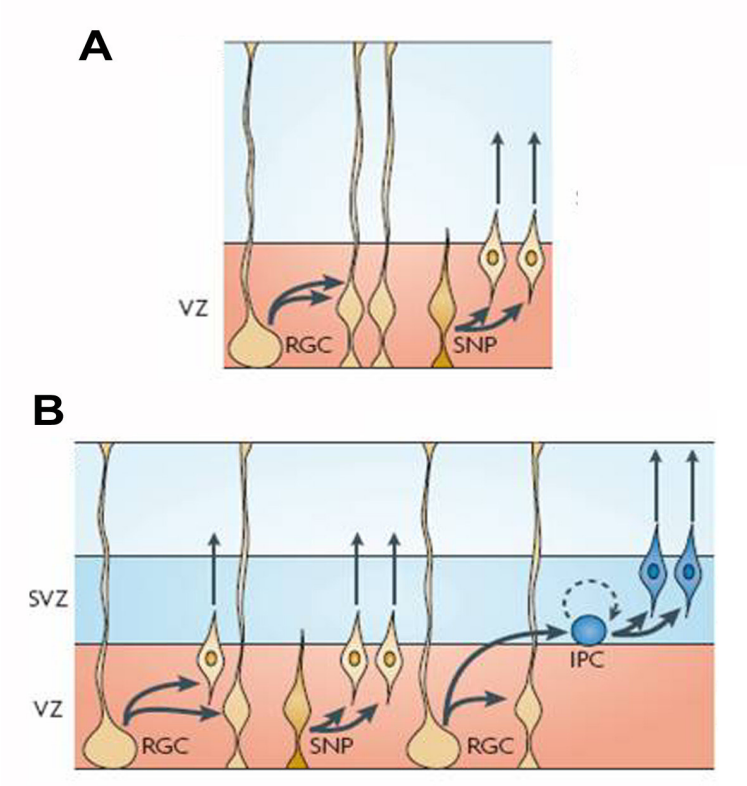


**Figure 4. Proliferative behaviour of cortical progenitor.** Schematic transects of the rodent cortex at embryonic day 13 (E13) **(A)** and at E17 **(B)**. Cortical neurons are generated from three types of precursors: radial glia cells (RGCs), short neural precursors (SNPs) and intermediate progenitor cells (IPCs). RGCs and SNPs divide at the apical surface of the ventricular zone (VZ). RGCs undergo several types of symmetrical and asymmetrical divisions, as indicated by the arrows, including self-renewing ones **(A)** or neurogenic divisions **(B)**. SNPs are committed neural precursors. IPCs divide away from the ventricular surface in the VZ and in the subventricular zone (SVZ) **(B)**. IPCs have been reported to undergo mostly neurogenic divisions with a small fraction undergoing symmetrical proliferative divisions (as indicated by the dotted circular arrow). Through asymmetrical divisions, RGCs give rise to IPCs that migrate to the SVZ. Adapted from Dehay and Kennedy (2007).

After neurulation, and before neurogenesis gets under way, the neural tube is composed of a single layer of radially arranged bipolar cells, which divide symmetrically originating two identical progenitors and thereby increasing their number. These cells are highly polarized along their apical–basal axis (Rakic, 1995; Malatesta et al., 2008). The organization of their plasma membrane presents both tight junctions and adherens junctions at the lateral-apical end. Even if the cells of such epithelium span the entire thickness of the neural tube they look layered (‘pseudostratified’), this because those nuclei migrate up and down the apical–basal axis during the cell cycle (interkinetic nuclear migration) (Gotz and Huttner, 2005; Kosodo and Huttner, 2009). As development proceeds, around E9-E10 in the mouse telencephalon, epithelial cells in

neural tube undergo some changes in their gene expression pattern, cytological characteristics and differentiation potential., There is the induction of the intermediate filament nestin and of the related antigen recognized by the antibody RC2; besides the occludin (a tight junction component) is downregulated and the apical junctional complex, in such way, loses its previous role as a permeability barrier giving rise the permeability changes; finally, the dependency of junctions on Notch signaling becomes evident (Frederiksen and McKay, 1988; Edwards et al., 1990; Aaku-Saraste et al., 1996). Starting from this stage, the cells can be considered properly "neuroepithelial progenitor" (Malatesta et al., 2008). NEPs maintain the interkinetic nuclear migration, which involves their entire soma till the basal membrane, and divide mainly symmetrically on the luminal surface of the neural tube (Kosodo et al., 2004; Rakic, 1995). From this stage, however, an increasing number of cells start to divide asymmetrically, giving rise to another neuroepithelial cell and either to a neuron or, alternatively, to a progenitor cell that will undergo mitosis at a significant distance from the ventricular surface (basal progenitor or IPC) (Haubensak et al. 2004, Pontious et al., 2008). In this way neuroepithelium transforms into a tissue with numerous cell layers (Malatesta et al., 2008). Shortly after the appearance of the first neurons, NEPs undergo a second change in their characteristics acquiring molecular and cytological features typical of the astroglial lineage such as expression of lipid-binding protein BLBP, astrocytic glutamate transporter GLAST and calcium-binding protein S100β (Feng et al., 1994; Shibata et al., 1997; Malatesta et al., 2000; Hartfuss et al., 2001; Vives et al., 2003), accumulation of glycogen granules in the cytoplasm; at this stage NEPs loose certain epithelial features, like tight junctions (but not adherens junctions), and the apical-versus-basal polarity delivery of certain plasma-membrane proteins (Aaku-Saraste et al., 1996; Aaku-Saraste et al., 1997). In essence, after the onset of neurogenesis, NEPs give rise to the radial glial cells RGCs, a distinct, but related, cell type (Gotz and Huttner, 2005; Malatesta et al., 2008). RGCs represent more fate-restricted progenitors than NEPs and successively replace those (Malatesta et al., 2000). In mice these changes occurs throughout most of the brain between E10 and E12. However RGCs still exhibit residual neuroepithelial properties such as the presence of markers like the intermediate-filament protein nestin, the maintenance of an apical surface and important features of apical–basal polarity such the presence of adherens junctions, and the basal lamina contact. Like NEPs, RGCs show interkinetic nuclear migration, although nuclei do not migrate through the entire length of the cytoplasm, and mitosis occurred at the ventricular edge of the neural tube (Hartfuss et al., 2001; Gotz and Huttner, 2005). RGCs have long been known to have crucial roles in guiding neurons to their final locations in the cortical plate by serving as migratory scaffolding (Rakic, 2003; Noctor et al. 2004). RGCs function as progenitors that make

major contributions to cortical neurogenesis by generating pyramidal neurons, either directly through mitoses at the apical surface of the VZ, or indirectly through the production of proliferating intermediate progenitors (Malatesta et al., 2003). The majority of RGCs go through asymmetric divisions, giving rise two distinct daughter cells: neurogenic divisions (producing a neuron and a self renewal RGC), asymmetric progenitor divisions (producing a RGC and a IPC migrating away from the ventricle re-entering the cell cycle), final radial glia divisions (both the daughter cells migrate away from the ventricle). A minority of RGCs go through symmetric division in which a RGC generate two RGCs that both remained in the VZ and subsequently divided. Such type of division occurs frequently during early stages of cortical neurogenesis in order to expand the proliferative population (Noctor et al. 2004). In addition to the full-length radial glia, other neuron-producing precursors have been described as apical precursor in the VZ (Gal et al., 2006; Ochiai et al., 2007). These studies observed a subpopulation of progenitors that can be distinguished from radial glial cells by the absence of a full-length pial process and by the ability to drive transcription from the Tα1 α-tubulin promoter. In these studies they named them as 'short neural precursors' (SNP) or pin-like cells. SNPs are labeled with markers that had been considered radial glia specific; they are proliferating group of progenitors that can undergo at least one full cell cycle while in the VZ (Gal et al, 2006).

Intermediate progenitor cells (also known as basal progenitors) originate from asymmetric divisions of NEPs and RGCs (and possibly by SNPs). These cells lost their contact with both apical and basal surface and, concomitantly with the migration of their nucleus to the basal side of the ventricular zone, settled in more basal position of VZ giving rise the subventricular layer (SVZ). In the mouse, the SVZ starts to form at E13.5 and expands significantly during late corticogenesis. IPCs divide at basal positions in the developing neocortex and produce pairs of neurons (indirect neuronogenesis) or pairs of IPCs by limited mitotic symmetric division (1-3 cycles) (Englund et al. 2005, Pontious et al. 2007, Kowalczyk et al. 2009). As opposed to apical proliferative layers, IPCs are also distinguishable by low-level or completely missing expression of key transcriptional regulators implicated in RGC self-renewal, including Pax6 and Emx2. Moreover, they express Tbr2/Eomes (which is confined to IPCs, but not to their cortical progenies), Cux1-2, and non coding RNA *SVET1* (Heins et al., 2002; Molyneaux et al. 2007). Furthermore, IPCs present multipolar morphology, multipolar mode of cell migration and neuronal restriction of daughter cell fates. It has been proposed that IPCs contribute to all cortical layers and influence mainly laminar thickness (Pontious et al., 2007). Nevertheless other model suggests IPCs contribution exclusively to upper layer cortical neurons (Tarabykin et al., 2001;

Cubelos et al., 2007). Throughout the corticogenesis, apical progenitor divisions (RGCs, NEPs and SNPs) outnumber basal divisions (IPCs) (Kowalczyk et al. 2009).

| | NE | RG | SNP | IPC |
|---|---|---|---|---|
| Ages | E9.5–E13.5 | E11.5–P0.5 | E12.5–E16.5 | E10.5–P0.5 |
| Morphology | radial | radial | radial (VZ only) | multipolar (few radial) |
| Migration | IKNM | IKNM | IKNM | multipolar |
| Mitosis | apical | apical | apical | basal (rare apical) |
| Mitotic cycles | unlimited | many (≥10) | n.d. | 1–3 |
| Daughter cell fates | NE, RG, IPC, N | RG, IPC, N | SNP, N | IPC, N |
| Molecular expression | prominin 1 (CD133), nestin | Pax6, tenascin-C, BLBP, vimentin, nestin, GLAST | tubulin $\alpha_1$ promoter | Tbr2 (some low-level Pax6) |
| Abundance | 0–100% depending on age | approx. 50% of VZ progenitors (E13.5–E16.5) | approx. 50% of VZ progenitors (E13.5–E16.5) | 10–50% of all progenitors (E10.5–P0.5) |

**Table 1. Neurogenic progenitor cells in embryonic mouse cerebral cortex.** BLBP brain lipid-binding protein; GLAST astrocyte-specific glutamate transporter; IKNM interkinetic nuclear migration; N neuron; n.d. not determined; P postnatal day. Adapted from Pontious et al. (2007).

Nevertheless using *Tis2*-GFP mice, in which GFP is expressed only in neurogenic division, it has been demonstrated that among E10.5 to E18.5, the neurogenic fraction of basal divisions remained much higher (between 40% and 80%) than the neurogenic fraction of apical divisions (between 10% and 20%). Only at the end of neurogenesis, on P0.5, did the neurogenic fraction of RGCs approach that of IPCs (converging to 30-55%), consistent with terminal neurogenesis (Kowalczyk et al., 2009). This study indicated that, despite the numerical predominance of RGCs divisions, even during preplate neurogenesis on E10.5-E11.5, IPCs actually produced the majority (>80%) of cortically derived projection neurons at all ages.

## 1.5 Spatio-temporal regulation of proliferative-differentiative kinetics: the role of classical polypeptide-encoding genes.

Kinetics of neuronal generation emerges as a result of different basic morphogenetic subroutines, such as precursors proliferation, precursors death, transitions among distinct proliferative compartments, cell cycle exit, post-mitotic neuronal differentiation, cellular migrations. Molecular aspects of such process have been deeply studied in last decades and, even if different points still need to be clarified, at the moment the state of the art has been summarized in different reports (Baehrecke, 2002; Gotz and Huttner, 2005; Guillemot 2006; Dehay and Kennedy 2007; Molyneaux et al. 2007; Caviness et al., 2008; Rakic et al., 2009). Control of these subroutines is extremely complex and, until now, a large number of polypeptide-encoding genes belonging to distinct structural and functional families have been implicated in it. Gradients of extracellular signalling molecules such as sonic hedgehog,

fibroblast growth factors and bone morphogenetic proteins are key regulatory factor during the specification of the cortical primordium (Rallu et al, 2002). Many transcription factors have a crucial role during early cortical development including Foxg1, Gli3, Lhx2, Emx2 and Pax6. These establish the neocortical progenitor domain by repressing dorsal midline (Lhx2 and Foxg1) and ventral fates (Emx2 and Pax6) (reviewed in Molyneaux et al., 2007) and also are essential for generating and maintaining the dorsal and ventral subdivisions of the telencephalon (Reviewed in Herbert and Fishell, 2008). The transcription factors Emx2, Pax6 and Sox2 are fundamental for RGCs self renewal (Muzio et al., 2002; Bani-Yaghoub et al., 2006). Contrary the key transcription factors Tbr2, Cux1, Cux2 and *Svet1* are present in IPCs and have an active role for the right morphogenesis of the SVZ (Sessa et al., 2008; Cubelos et al., 2008; Tarabykin et al., 2001). Among them Pax6 and Tbr2 have been largely used as markers for, respectively, apical and basal, proliferative compartments (Englund et al., 2005). Transcription factors may maintain a proliferating progenitor state, as in the case with the Hes and Id families of bHLH factors (Ross et al. 2003). Otherwise they can promote exit from cell cycle and panneuronal as well as subtype-specific differentiation programs: this is the case of proneural genes such as Ngn1, Ngn2 and Mash1 (Bertrand et al. 2002). Proteins of the Delta-Notch signalling including receptor, ligands, modulator and effectors are involved on the maintenance of the progenitor state (reviewed in Yoon and Gaiano, 2005). Finally, Reelin, a protein express by Cajal-Retzius cells in MZ, has been demonstrated to be indispensable to form a stereotypical inside-out and six-layered pattern interacting with Notch signalling in regulating neuronal migration (Tissir and Goffinet, 2003; Hashimoto-Torii et al., 2008). Apart from Reelin, different species of polypeptide-encoding genes are involved during radial and tangential neural migration process (LoTurco and Bai, 2006; Huang, 2009).

In addition to polypeptide-encoding mRNAs, a huge number of so-called non-coding RNAs (ncRNAs) are expressed in the developing central nervous system (CNS). Their expression patterns and their functions are presently subject of deep experimental investigation (Amaral and Mattick, 2008).

### 1.6 Non-coding genes: brief classification

The numbers of protein-coding genes and the extent of protein coding sequences do not change appreciably across the vertebrates despite large differences in developmental complexity (Taft et al., 2007). Besides, the notion that phenotypic divergence and specialization in organisms result from alterations in regulatory circuits rather than ‘‘chemical structures’’ of proteins dates back to the early years of molecular biology (Britten and Davidson, 1969).

Information underlying development lies in regulatory elements which define different gene expression programs whose in turn define specific phenotypes: this is also largely the basis for phenotypic heterogeneity between species and individuals (Wray, 2007). It is well known that untranslated regions (UTRs) in mRNAs, intronic and intergenic nonprotein-coding sequences, increase dramatically in size with the increasing developmental complexity in eukaryotes, suggesting that these sequences contain a greatly expanded regulatory framework to control gene expression during differentiation and development (Taft et al. 2007). These regulatory sequences include *cis*-acting elements that control transcription (core promoter sequences, enhancers, silencers, insulators, and locus control regions), mRNA processing, localization, translation, and stability (splicing elements, UTRs, polyadenylation signals, and other regulatory motifs). The fact that a great measure of the entire genome of all eukaryotes is in fact transcribed, generate an enormous number of RNAs that have little or no protein-coding potential, increasing the complexity of such regulatory framework (Carninci et al., 2005).

So far important evidence suggest that much of the expanded regulatory information in eukaryotes is transacted by a kind of ncRNAs which are different from the well-characterized ones which perform infrastructural and housekeeping roles (such as rRNAs, tRNAs, and snRNAs). These ncRNAs control gene expression at various levels, including chromosome dynamics, chromatin architecture, transcription, post-transcriptional processing, and translation, focusing primarily on animals (Amaral and Mattick, 2008). Emerging data increasingly suggest that a protein-centric view of the mammalian genome is simplistic and that much of the information that programs mammalian development lies within this previously hidden layer of noncoding RNA-regulatory networks (Mattick, 2007).

ncRNAs have been identified as -*cis* and *trans*-acting regulators of development and can operate by many different mechanisms at transcriptional or post-transcriptional level regulating translation, mRNA stability and processing. Different reports also demonstrate the important role of ncRNAs in control of chromatin architecture and epigenetic processes directing generic chromatin-modifying enzymes and complexes to their sites of action and regulating those pathways (reviewed in Amaral and Mattick, 2008).

At structural level ncRNAs are classified in two main categories that are long ncRNAs (LncRNAs, which are transcripts of length >200 base pairs) and small ncRNAs (SncRNAs, which are transcripts of length <200 base pairs). LncRNAs can be placed into one or more of five further broad categories: (1) sense, or (2) antisense, when they overlap one or more exons of another transcript on the same, or opposite, strand, respectively; (3) bidirectional, when its expression is regulated by a bidirectional promoter (in these case their transcriptional events, and

those for neighboring transcripts from opposite strand, are initiated in close genomic proximity), (4) intronic, when it is derived wholly within an intron of a second transcript, or (5) intergenic, when it lies within the genomic interval between two genes (Ponting et al., 2009). Transcription of LncRNAs can regulate the expression of genes in close genomic proximity (*cis*-acting regulation), as in the case of X chromosomes inactivation in female *Xist* (Brockdorff et al., 1992) and when associate with parental imprinting (Sleutels et al., 2002), otherwise the transcription of LncRNAs can target distant transcriptional activators or repressors (*trans*-acting regulation) via a variety of mechanisms such as ‘‘transcriptional interference’’ (Martens et al., 2005), modifying the accessibility of protein-coding genes to RNA polymerases (Hirota et al., 2008) and binding to DNA or RNA-binding proteins (Wang et al., 2008). On the other hand, SncRNAs are generally processed from different types of large RNA precursors that are cleaved by generic complexes containing proteins of the RNAse III family which collectively generate small RNAs that regulate gene expression and other aspects of genome physiology (Stefani and Slack, 2008). SncRNAs comprise various subclasses that differ in their biogenesis pathways, characteristic sizes, protein-binding partners and functions (Amaral and Mattick, 2008). The most intensely studied class of small RNAs in eukaryotes are the microRNAs (miRNAs). They are 22-nt molecules produced from imperfect hairpin structures present in LncRNAs precursors, or introns of noncoding and protein coding genes (Winter et al., 2009), which will be deeply considered subsequently in a separate section.

Short interfering RNAs (siRNAs) have a distinct size distribution, in any case around 21-bp long, but in contrast to miRNAs, which are excised in a precise way from their dsRNA precursor, siRNAs are directly processed by Dicer, a cytoplasmatic RNAse III complex, in a more random fashion (Elbashir et al., 2001). siRNAs can be produced from RNA transcribed in the nucleus (endogenous siRNAs), otherwise can be virally derived or experimentally introduced as chemically synthesized dsRNA (exogenous siRNAs) (Farazi et al., 2008). In plant endogenous siRNAs can be further subdivided in subclasses on the bases of their biogenesis. They include antisense-siRNAs (natsiRNAs), trans-acting-siRNAs (tasiRNAs) and heterochromatic small RNAs (hcRNAs). natsiRNAs are endogenously expressed siRNAs that originate from overlapping sense and antisense transcripts (Borsani et al., 2005). tasiRNAs are generated from specific non-coding genomic regions as primary single strand RNA which is cleaved in little fragments by Ago1 (miRNAs machinery protein). Such fragments are used by a RNA-dependent RNA polymerase (RdRP) as templates for dsRNA synthesis which are cleaved by a Dicer RNAse to yield 21 nt tasiRNAs (Vazquez, 2006). Both natsiRNAs and tasiRNAs guide mRNA degradation (Adenot et al. 2006). hcRNAs are mostly derived from repeat-associated genomic

regions and have been identified also in yeasts, playing a role in heterochromatin regulation (Farazi et. al. 2008). Endogenous siRNAs have also been identified in C. elegans as tiny-noncoding RNA (tncRNA). tncRNAs are ~22 nts in length, they depend on Dicer for their biogenesis, and derive from non-coding, non-conserved sequences. The function of tncRNAs has not yet been elucidated (Yigit et al., 2006). So far, endogenous siRNAs have not been identified in mammals or insects (Farazi et al. 2008). Nevertheless in cultured mammalian cells, siRNAs have been successfully used to analyze gene function (Elbashir et al., 2001b). The exposure of mammalian cells to long dsRNA induces an antiviral interferon response that leads to apoptosis. For such reason endogenous siRNAs are thought to play an important role in defending genomes against transgenes and transposons, as well as against foreign nucleic acids, such as viruses (Dorsett and Tuschl, 2004). This reaction can be bypassed by using siRNA duplexes that resemble in size and structure the miRNA processing intermediates (Liu et al., 2004).

PiwiRNAs (piRNAs) are another class of SncRNAs. piRNAs are 28 to 33 nt in length characterized by their association with Piwi protein family (O'Donnell et al, 2007). In mammals, piRNA biogenesis is thought to be Dicer independent resulting from single-stranded transcripts which are not usually derived from repeat sequences (Vagin et al, 2006; Betel et al, 2007).

| Class | Size (nt) | Structure of precursor | Mechanism of action | 3' End modifications | Organism |
|---|---|---|---|---|---|
| miRNA | 20-23 | Imperfect hairpin | Translational repression, mRNA cleavage | Unmodified | Mammals |
| | | | | Unmodified | Insects |
| | | | | Unmodified | *D. rerio* |
| | | | | 2'-O-methylated | Plants |
| | | | | Unmodified | Nematodes |
| | | | | Modified, but uncharacterized | *C. reinhardtii* |
| | | | | | Viruses |
| siRNA | 20-23 | dsRNA | mRNA cleavage | Unmodified | Mammals |
| | | | 2'-O-methylated | Insects | |
| | | | | Uncharacterized | *D. rerio* |
| | | | 2'-O-methylated | Plants | |
| | | | | Unmodified | Nematodes |
| | | | | Uncharacterized | *S. pombe* |
| | | | | Uncharacterized | *N. crassa* |
| | | | | Uncharacterized | *T. brucei* |
| | | | | Modified, but uncharacterized | *C. reinhardtii* |
| tasiRNA | 21-22 | dsRNA | mRNA cleavage | 2'-O-methylated | Plants |
| natsiRNA | 21-22 | dsRNA | mRNA cleavage | 2'-O-methylated | Plants |
| Secondary siRNA | 20-25 | dsRNA | mRNA cleavage | Unmodified | Nematodes |
| | | | | 2'-O-methylated | Plants |
| tncRNA | 22 | Uncharacterized | Uncharacterized | Uncharacterized | Nematodes |
| hcRNA | 24 | dsRNA | Regulation of chromatin structure | 2'-O-methylated | Plants |
| | | | | Uncharacterized | *S. pombe* |
| | | | | Uncharacterized | *T. brucei* |
| rasiRNA | 23-28 | Putative ssRNA | Regulation of chromatin structure | 2'-O-methylated | Insects |
| | | | | 2'-O-methylated | *D. rerio* |
| piRNA | 28-33 | Putative ssRNA | mRNA cleavage (in vitro evidence) | 2'-O-methylated | Mammals |
| | | | | 2'-O-methylated | Insects |
| | | | | 2'-O-methylated | *D. rerio* |

**Table 2. Classes of small RNAs and their characteristics.** hcRNA, heterochromatic small RNA; miRNA, microRNA; natsiRNA, endogenously expressed siRNA that originates from overlapping sense and antisense transcripts; piRNA, Piwi-interacting small RNA; rasiRNA, repeat-associated-siRNA; siRNA, small interfering RNA; tasiRNA, trans-acting siRNA; tncRNA, tiny-noncoding RNA. Adapted from Farazi et al. (2006)

Unlike miRNAs, piRNAs are not processed in a precise manner since tens of thousands of distinct piRNAs generated from the 50 to 100 defined primary transcripts (Watanabe et al. 2006). Mammalian piRNAs are strongly expressed in the male germline (about 10-fold higher than the miRNAs content of these cells) (Aravin et al., 2006). Although the targets of piRNAs and their mechanism of action are largely unknown, some reports demonstrated them role in spermatogenesis and transposons regulation in mammal (O'Donnell and Boeke, 2007). rasiRNAs found in *D. melanogaster* and *D. rerio* have been thought to belong to the piRNA class since their association with members of the Dicer independent-Piwi family, and because their length ranging between 23 and 28 nt (Vagin et al., 2006). rasiRNAs play a crucial role in controlling the expression of homologous sequences dispersed throughout the genome (O'Donnell and Boeke, 2007).

### 1.7 miRNAs: biogenesis and functions

miRNAs are short (20-23 nt), endogenous, single-stranded SncRNAs molecules abundant in animals, plants and even in virus. miRNAs regulate gene expression using base-pairing to guide RNA-induced silencing complexes (RISC) to specific mRNA with fully o partly complementary sequence (Bartel, 2004; Cullen, 2007). The miRNA processing pathway has long been viewed as linear and universal to all mammalian miRNAs as a "canonical" way (fig. 5). Such canonical biogenesis includes the production of a primary miRNA transcript (Pri-miRNA) with stem-loop regions by RNA polymerase II, but occasionally by RNA polymerase III, and cleavage of the Pri-miRNA by the microprocessor complex RNase III Drosha–DGCR8 (Pasha) in the nucleus (Lee et al., 2004; Borchert et al. 2006). The resulting precursor hairpin, the pre-miRNA, is exported from the nucleus by Exportin-5–Ran-GTP (Yi et al., 2003). In the cytoplasm, the RNase III Dicer in complex with the double-stranded RNA-binding protein TRBP cleaves the pre-miRNA hairpin to its mature length (Bernstein et al. 2003). The functional strand of the mature miRNA is then loaded together with Argonaute (Ago2) proteins into the RNA-induced silencing complex (RISC), guiding RISC to silence target mRNAs through mRNA cleavage, translational repression or deadenylation, whereas the passenger strand is degraded (Bartel, 2004; Winter et al., 2009). Nevertheless, far from following a few simple rules of production and action, miRNAs show diverse features that do not obey to a simple classification.

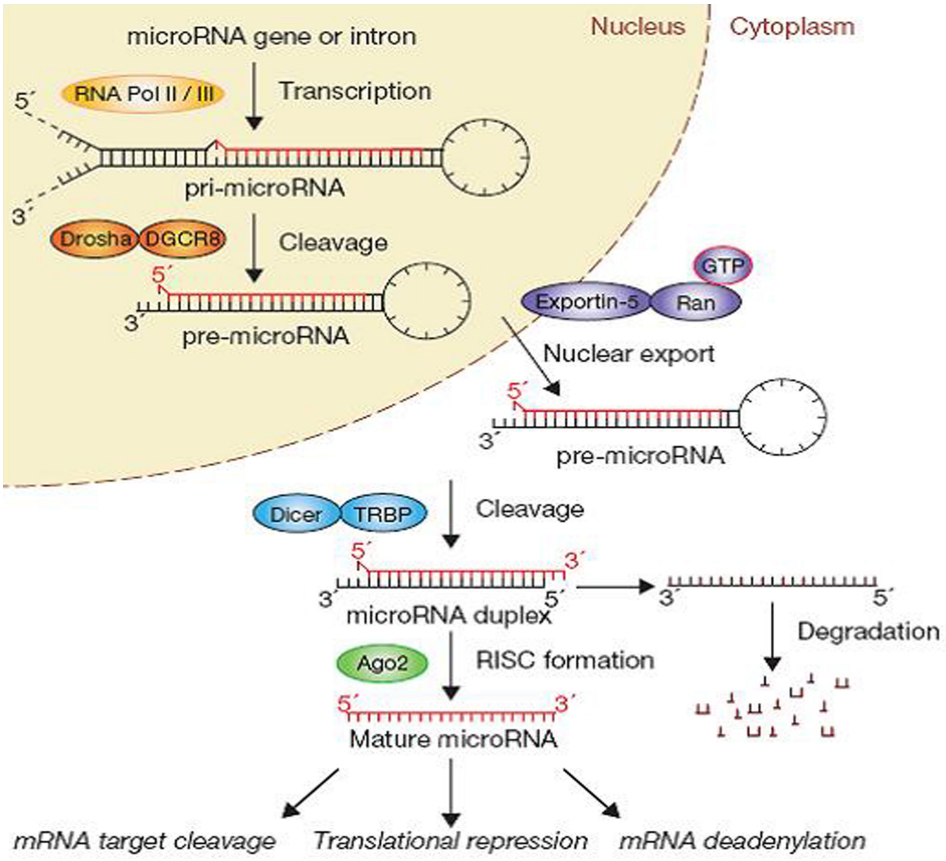


**Figure 5. The "linear" canonical pathway of microRNAs processing.** Adapted from Winter et al. (2009)

Primary miRNA transcripts are usually polyadenylated and capped (hallmark of Rna polymerase II transcription), although miRNA derived from RNA polymerase III primary transcript have been found (Borchert et al. 2006). Their transcription can be differently regulated according to promoter and terminator elements. In some case organization in cluster facilitate a wide variety of regulation (Lujambio et al., 2008: O'Donnel et al., 2005). Moreover editing (a process defined as transcriptional change of RNA sequences by deamination of adenosine (A) to inosine (I), altering the base pairing and structural properties of the transcript) on different Pri-miRNA transcript has been documented (Luciano et al., 2006; Yang et al. 2006). Such miRNA editing can influence processing at multiple steps (Dicer and Drosha) or can change the miRNA complementarity to target sequences, increasing the diversity of the cellular miRNA pool (Kawahara et al. 2007a; Kawahara et al., 2007b). The RNase III Drosha cleaves the 5' and 3' arms of the pri-miRNA hairpin giving rise to a stem and loop with a 5' phosphate and 2 nt at 3' overhang. Instead, DGCR8 determines the cleavage site which is 11 bp (one turn of dsRNA helix) far away from the stem-loop region (Han et al., 2003; Zeng et al., 2006). Drosha-mediated cleavage of pri-miRNAs can take place co-trancriptionally preceding splicing of the host RNA which contains the miRNAs, since splicing is not inhibited by Drosha-mediated cleavage

(Morlando et al. 2008; Kim et al., 2007). The production of Pri-miRNAs can be subject to specific regulation according to the processed miRNAs and the cell type. Recently it was shown that Drosha-DGCR8 complex can bind helicases, double stranded RNA binding proteins and ribonucleoproteins which expression levels and activity can be in turn regulated. These interactions can affect the levels of some specific microRNA in certain conditions (Gregory et al., 2004; Fukuda et al. 2007; Michlewski et al. 2008; Davis et al., 2008). Moreover it has been also proved that miRNAs can be released from their host transcript after splicing via Drosha-independent through the action of the splicing machinery (Ruby et al., 2007; Berezikov et al., 2007). Other reports underline that Lin-28, a stem-cell-specific regulator (Darr and Benvenisty, 2009), can modify the activity of the microprocessor on specific microRNAs (fig. 6A) (Viswanathan et al., 2008). A correct processing of Pri-miRNAs, giving rise a Pre-miRNAs of a defined length with a stem-and-loop structure and the 3´ overhangs, is important for successful binding to Exportin-5. This structure control ensures the export into cytoplasm of only correctly processed pre-miRNAs (Lund et al., 2004; Bohnsack et al. 2004). Cytoplasmatic Pre-miRNAs processing is mediated by a multi-protein complex "RISC loading complex" (RLC). RLC is composed of the RNase III Dicer, the RNA binding proteins Tar (TRBP) and PACT, and the RNAse Argonaute2 (Ago2) which is also part of RISC complex (Macrae et al., 2008; Winter et al., 2009). Pre-miRNAs, displaying high degree of complementarity along the hairpin stem, go through a first cleavage mediated by Ago2 on the prospective passenger strand producing the Ago2-cleaved precursor miRNA (ac-pre-miRNA) (Diederichs et al. 2007). Following the RLC formation, the RNase III Dicer cleaves the loop of the pre-miRNA, or the nicked ac-pre-miRNA, and generates a 21-23 nt miRNA duplex with two nucleotides protruding as overhangs at each 3´ end (Fig. 6B) (Bernstein et al., 2003). Additional mechanisms that regulate Dicer activity, specifically for some microRNAs, have been found in different organisms (Obrnosterer et al. 2006; Rybak et al. 2008; Li et al., 2005). After the Dicer mediated cleavage, the RLC is disassembled by the dissociation of Dicer, TRBP and PACT from RISC. The microRNAs double strand duplex is then unwound into the functional guide strand, which will be retained into the active RISC, and a passenger strand, which is subsequently degraded. Although different helicases have been linked to the miRNA pathway such process has not been fully elucidated (Salzman et al. 2007). It has been proved that in ac-pre-miRNA the unwinding process is facilitated (Diederichs et al., 2007). Strand retention is based on the relative thermodynamic stability of the duplex's ends. Usually, the 5' terminus of the retained strand is the less stable base paired end of the duplex (Kim, 2005). The degree of miRNA-mRNA complementarity, based on the seed sequence of the miRNA (2-8 nt from the 5' end), has been considered a key

determinant of the regulatory mechanism (Bartel, 2004). In fact RISC can silence targets mRNAs through mRNA translational repression or cleavage. Repressed initiation of elongation, destabilization of PolyA tail, and promotion of ribosome dissociation from the target mRNA are mechanisms through which RISC inhibit translation on target mRNA. RISC give rise to an Ago-catalyzed mRNA cleavage in case of high complementarity among seed sequence of miRNAs and target mRNA (Carthew et al., 2009). In any case the mRNA target site accessibility, influenced by stable secondary structure and by association of RNA binding proteins, can alter the miRNAs effect (Kertesz et al., 2007). Potential miRNAs target site have been mainly found into 3'UTR of target transcript (Carthew and Sontheimer, 2009), even if miRNAs guided repression has been found also in 5'UTR and ORF of mRNAs (Lytle et al., 2007; Forman et al., 2008). In some case, in mammals, microRNAs have been found localized mainly into the nucleus (Kim et al., 2008). It has been suggested that a hexanucleotide element, transferable nuclear localization motif, act as *cis*-acting regulatory sequence (Hwang et al., 2007). Re-import of miRNAs into the nucleus open the possibility that miRNAs could regulate gene expression at the transcriptional level (Place et al., 2008).

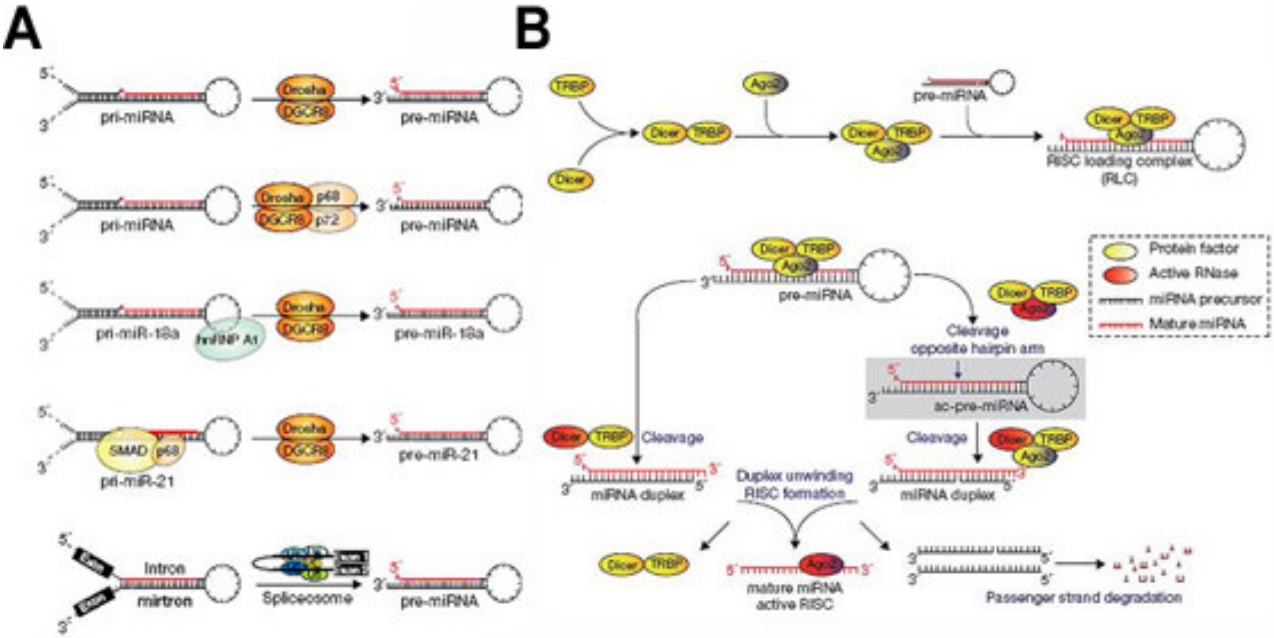


**Figure 6**. **Regulation of pri-miRNA processing and generation of the additional intermediate, the ac-pre-miRNA. (A)** Different modulation of the pri-miRNA processing: microprocessor complex Drosha–DGCR8 cleaves the pri-miRNA, releasing the pre-miRNA, some miRNAs require additional specificity factors for efficient cleavage, interaction of pri-miR-18a with hnRNP A1 which facilitates cleavage of this specific miRNA by Drosha, TGF-β signalling induces SMAD binding to the miR-21 precursor enhancing its efficient processing by Drosha. Splicing can also replace Drosha processing if the released and debranched intron (mirtron) has the length and hairpin structure of a pre-miRNA. **(B)** Dicer and TRBP interact before Ago2 is recruited to form a ternary complex that binds to the exported pre-miRNA constituting the RISC loading complex (RLC); after, pre-miRNA binding, Dicer releases the mature miRNA duplex. For some miRNAs, however, Ago2 cleaves first the prospective passenger strand, generating a nicked hairpin called ac-pre-miRNA or Ago2-cleaved pre-miRNA. Adapted from Winter et al. (2009).

The role of microRNAs during development has been largely documented (Stefani and Slack, 2008). In nematodes different miRNAs are key factors controlling switch among heterocronic developmental stages (Flynt and Lai, 2008; Lee et al., 1993). In these cases miRNAs act as genetic switch where the miRNA and its target protein are only transiently co-expressed. Often, several miRNAs, which work as genetic switches, are involved in bistable loops with their targets that, in turn, encode regulators of miRNAs expression or activity (Li and Carthew 2007; Chang et al., 2005; Kim et al. 2007).

Nevertheless miRNAs can be co-expressed with their targets modulating the threshold activity of target transcripts in a "Tuning" or "De-Noising" fashion (Lai, 2002; Karres al., 2007). Since microRNAs can also regulate large numbers of targets (Baek et al., 2005; Selbach et al., 2008) they become fundamentals during the control of spatial-temporal global changes occurring in a given cell or organ (Giraldez et al., 2006; Lim LP et al. 2005). Besides, miRNAs can work as reversible regulators; this because they can act as translational repressors without give rise to an irreversible target cleavage open the possibility of targets mRNA reactivation. Such strategy is advantageous in situations where the regulatory flexibility is fundamental as in stress conditions (Bhattacharyya et al. 2006), in polarized cells (Schratt et al., 2006) or in maternally deposited transcripts (Kedde et al., 2007). Finally, although miRNAs are thought as repressors, a potentially general role for miRNAs as direct gene activators has been defined (Vasudevan et al., 2007a; Vasudevan et al., 2007b) opening a new point of view about miRNAs functions.

Up till now studies on biosynthesis and functions of miRNAs highlight multiple pathways and mechanisms of biogenesis. These specific differences lead miRNAs to be part of many regulatory systems in animal developmental biology.

## 1.8 Thesis subject and work plan: expression pattern of miR-124 and miR-9 during early mouse cortical development, *in vitro* and *in vivo* miR-124 functional characterization

We focused our studies mainly on the expression and the role of microRNA 124 and microRNA 9 during early mouse cortical neurogenesis. We based our strategies on different reports which, mainly through screening studies on large scale, suggested a considerable role for these two microRNAs during early cortical development.

In mouse genome, both for miR-9 and miR-124, there are three loci which encode their hairpin precursors. Pri-miR-124(1) on chromosome 14, Pri-miR-124(2) on chromosome 3 and Pri-miR-124(3) on chromosome 2 encode for mir-124 precursors. As for miR-9, two copies of Pri-miR-9(1) as part of a larger duplicated region on mouse chromosome 3, Pri-miR-9(2) on chromosome

13, and Pri-miR-9(3) on chromosome 7 were found (Griffiths-Jones et al. 2006). miR-124 and miR-9 sequences are conserved between invertebrates and vertebrates (Lagos-Quintana et al. 2002). Cloning of MicroRNAs from low molecular weight RNA (LMW_RNA) and Northern Blot analysis accounted miR-124 for 25% to 48% of all mouse brain miRNAs; remarkably also miR-9 was noteworthy found in mouse brain tissue (Lagos-Quintana et al. 2002, Sempere et al. 2004). Moreover microarray analysis on LMW_RNA from rat brain tissue demonstrated that miR-124 increased more than 13-fold from E12 to E21, after which it remained stable, while miR-9 showed a similar pattern of up-regulation from E12 to E21 followed by down-regulation after birth and a steady-state level after P5 (Krichevsky et al. 2003, Thomson et al. 2004). These data were also validated by Northern Blot analysis (Krichevsky et al. 2003). Studies on D3-ES cell lines, P19 cell lines and mouse primary neural and astrocyte cultures demonstrated the exclusively neuronal identity of miR-124. On the other hand, depending on time in culture, an expression in both astrocytes and neurons was found for miR-9 (Smirnova et al. 2005). Microarray analysis of total Hela cells mRNA transfected with miR-124 RNA duplex for 12 and 24 hours gave a set of 174 genes downregulated by miR-124. One striking feature of this 174 genes is them expression at lower levels in the brain than in other tissues of the body: in a sense transfecting this brain miRNA into HeLa cells shifted HeLa gene expression towards that of brain (Lim et al. 2005). Besides whole mount *in situ* hybridization performed on zebrafish using the looked nucleic acid technology (LNA-Exiqon®) demonstrated a nervous system predominant presence of miR-124 and miR-9 (Wienholds et al. 2005). Finally, at the end of 2005, the presence of REST binding sites (Ballas et al. 2005) on all Pri-miR-9 and Pri-miR-124 promoters was demonstrated by Serial Analysis of Chromatin Occupancy (SACO). On the other side, it was proved the miR-124 sensitivity of the REST transcript, because of the presence of seed target sequence in the REST_3'UTR. In such report it was underlined how, in P19 cell lines and cultured neurons, miR-124 and REST act in a complementary way giving rise to a negative feedback loop (Conaco et al. 2006).

In the last few years, while this study was carried on, molecular mechanisms underlying miR-124 and miR-9 way of action were subject of intensive investigation. Different reports have been starting to elucidate the role of miR-124 and miR-9 during neurogenesis. Major findings coming from miR-9 gain of function studies include: a astroglial-to-neuronal shift of embryonic stem cells (ES cells) synergically induced with miR-124, probably due to hypophosphorylation of the glial lineage inductor STAT3 (Krichevsky et al. 2006); promotion of neurogenesis in the embryonic midbrain-hindbrain zebrafish domain, through a fine-tuning of the Fgf signaling pathway, so delimiting the organizing activity of the midbrain-hindbrain boundary (Leucht et al.

2008); stimulation of Cajal-Retzius cell differentiation by suppressing Foxg1 expression in mouse medial pallium, so giving rise to a regulation of Reelin-positive cells over the cortex (Shibata et al. 2008); inhibition of oligodendrocytes differentiation (Lau et al. 2008); *in vivo* acceleration of neural differentiation, via suppression of the nuclear receptor TLX, a promoter of neural stem cell proliferation and self renewal (Zhao et al. 2009). On the other hand, major findings coming from miR-124 gain of function studies include: stimulation of neuron-specific transcriptome splicing by targeting PTBP1 mRNA, which encodes a global repressor of neuron-specific pre-mRNA splicing normally active in nonneuronal cells (Makeyev et al. 2007); promotion of neurite outgrowth in differentiating P19 cells and mouse primary cortical neuron cultures (Yu et al. 2008); modulation of β1-integrin-dependent attachment of NSCs to the basal membrane in chick embryo (Cao et al. 2007); cross-talk with the general, anti-neuronal REST/SCP1 transcriptional machinery in chick embryo (Visvanathan et al. 2007); increased neuronal differentiation of adult rodent SVZ cells, by targeting the transcription factor Sox9 at the transition from the transit amplifying cell to the neuroblast stage (Cheng et al. 2009); in cooperation with miR-9*, modulation of the neuron-specific chromatin remodeling factor BAF53a in mammalian embryonic spinal cord (Yoo et al. 2009). Till now, however, the role of miR-124 in mammalian embryonic corticogenesis has been addressed *in vivo* only to partial extent. Makeyev et al. performed cross-correlation studies among expression of miR-124 and selected targets of it. Two studies (Makeyev et al. 2007; De Pietri-Tonelli et al. 2008) analyzed consequences of cortico-cerebral ablation of the whole miR machinery, following conditional *Dicer* knock-out. As previously mentioned, miR-124 functions were addressed *in vivo* also in the developing chick spinal cord (Cao et al. 2007; Visvanathan et al. 2007), however these studies led to some contrasting conclusions. Finally, a reduction of proliferation has been recently reported to occur in the mammalian embryonic spinal cord, upon combined miR-9*/miR-124 overexpression in neural precursors as documented by Crabtree and coll. (Yoo et al. 2009).

We illustrated the expression pattern of miR-124 and miR-9 in the developing mouse cortex, from E10 to early postnatal stages, using the LNA probes (Exiqon®). Besides, by integrated use of *in utero* electroporation of stage-specific reporter genes, immunofluorescence and LNA-oligo *in situ* hybridization technology, we deeply defined the of miR-124 expression timing among different cells compartments in the CNS primordium. Then, by *in vitro* lentivirus-based gene transfer and *in utero* electroporation of miR-124 expressing plasmids, we addressed the roles played by this molecule in regulation of embryonic cortico-cerebral neuronogenesis.

# 2. Results

## 2.1 miR-124 and miR-9 cortical expression patterns

We systematically studied the miR-124 and miR-9 expression pattern in the developing mouse cerebral cortex, by LNA-oligo *in situ* hybridization (Kloosterman et al. 2006).

No miR-124 signal was detectable in the cortex at E10.5, when, conversely this miRNA was strongly expressed by post-mitotic neurons of the ganglionic eminence (Fig. 7A). At E12.5, a light and diffuse signal was found throughout the cortical VZ and a stronger one within postmitotic neurons of the cortical preplate (Fig. 7B). The pattern became more complex at E14.5, when three distinct radial expression domains could be distinguished. A faint signal was still detectable within the VZ, an intermediate signal appeared in the SVZ, and a strong signal demarcated presumptive subplate (SP), cortical plate (CP) and marginal zone (MZ). Remarkably, a few intensely labeled cells could be also noticed at the VZ/SVZ border (Fig. 7C). This profile was basically retained at E16.5 and E18.5. At both these ages, miR-124 staining allowed to fairly distinguish the subplate from the cortical plate. Moreover, heavily labeled cells at the VZ/SVZ border became much more frequent. Finally, scattered cells, expressing miR-124 at high level, appeared in the VZ too (Fig. 7D, E). The miR-124 expression pattern turned sensibly simplified at P4, when the signal was restricted to the grey matter and was sensibly more intense in recently generated, layer 2-4 neurons (Fig. 7F). Remarkably, at all ages subject of investigation, miR-124 expression was tightly restricted to the CNS, being completely absent in the surrounding mesenchymal tissue (Fig. 8).

miR-9 is strongly expressed overall the cortical primordium at E 10.5 The signal increases in proximity of the cortical hem, confirming a possible action of miR-9 on the modulation of Cajal-Retzius cell differentiation in this site (Shibata et al. 2008) (fig. 9A). At E12.5, a strong signal was found throughout the cortex both in VZ and within postmitotic neurons of the cortical preplate. Interestingly, no signal was present in the diencephalon (Fig. 9B). At E.14.5 a strong signal was still present through the cortex, strengthened within the cortical plate (fig. 9C). At E16,5 the VZ and SVZ signal decreased while all postmitotic neurons in cortical plate and subplate retained a strong staining (fig. 9D). At E18,5 and at postnatal stages P4 and P15 the signal disappeared in SVZ and ependyma (E) while decreasing in postmitotic neurons in cortical plate (fig.9 E-G). At P4, miR-9 expression is more intense in upper than in lower cortical layers and at P15 it is detectable only in the latter ones (Fig. 9F,G). These data are consistent with what

Kosik and coll. found in the rat by northern blot: an up-regulation of miR-9 from E12 to E21, followed by down-regulation after birth and a stable expression after P5 (Krichevsky et al. 2003).

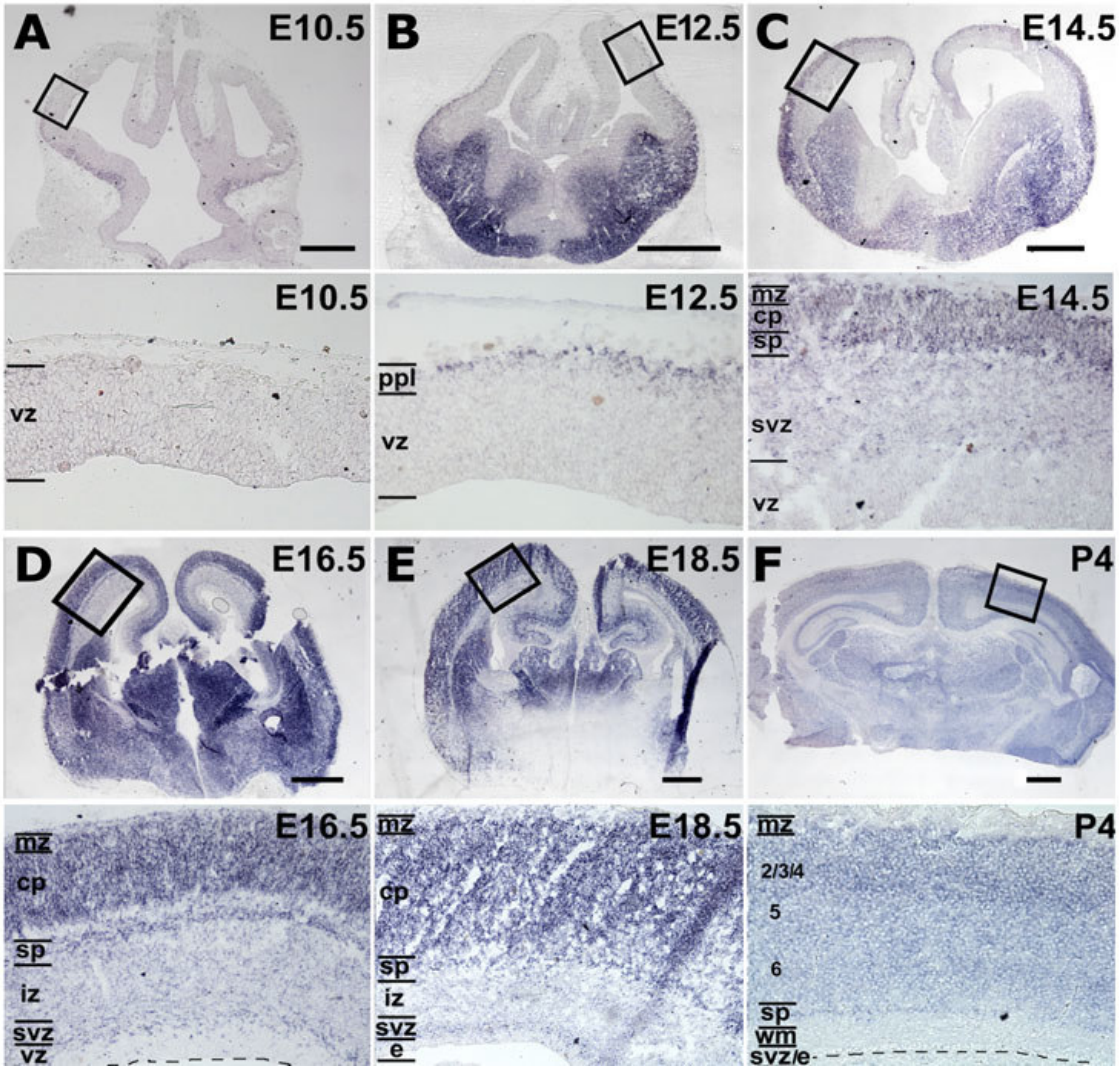


**Figure 7. Time course analysis of miR-124 expression.** (A-F) *In situ* hybridization of miR-124 on midfrontal E10.5-P4 mouse telencephalic sections. Magnifications of boxed areas are shown below each panel. Scale bars = 400 µm**.** Abbreviations: cp, cortical plate; e, ependyma; iz, intermediate zone; mz, marginal zone; ppl, preplate; sp, subplate; svz, subventricular zone; vz, ventricular zone; wm, white matter; 2/3/4,5 and 6 are cortical layers.

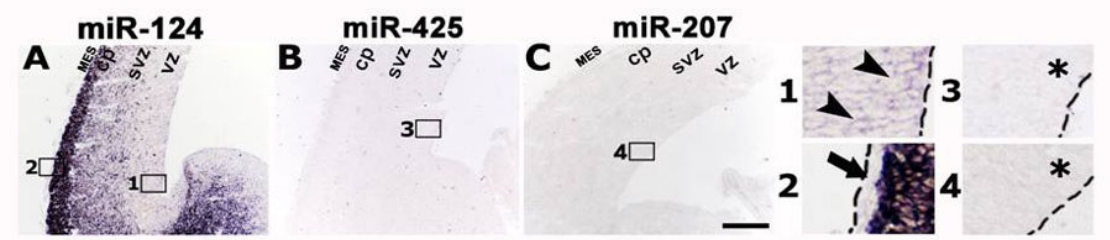


**Figure 8. Specific faint expression of miR-124 in the E14.5 VZ**. *In situ hybridization* of miR-124 (A), miR-425 (B) and miR-207 (C) probes on midfrontal E14.5 telencephalic sections. miR-425 and miR-207 are two microRNAs not expressed in the developing CNS (Lagos-Quintana et al. 2003, Landgraf et al, 2007 ). Magnifications of boxed areas illustrate the faint staining detectable in the VZ (black arrowheads) but not in mesenchymal tissue (black harrow) upon miR-124 hybridization, as well as the absence of any signal in samples hybridized with miR-425 or miR-207 (asterisks). Scale bar = 100 µm. Abbreviations: cp, cortical plate; svz, subventricular zone; vz, ventricular zone; mes, mesenchymal tissue.

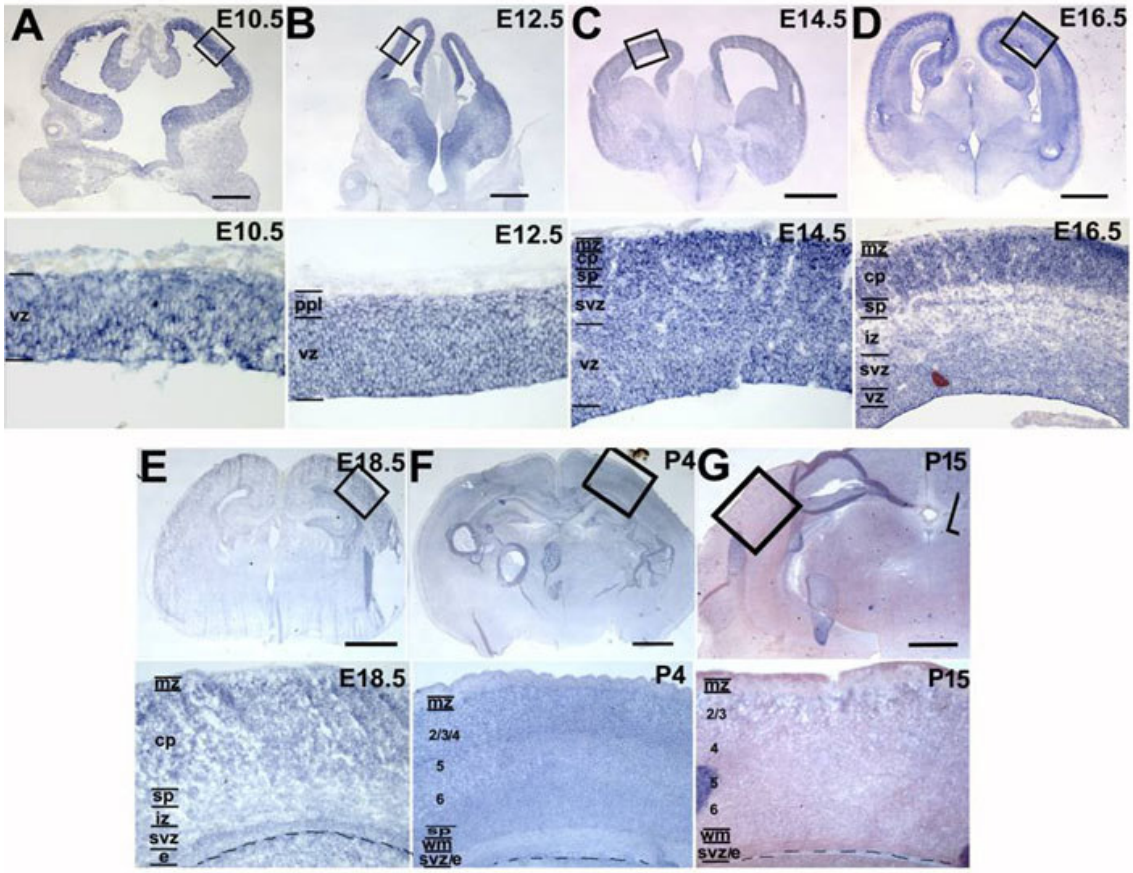


**Figure 9. Time course analysis of miR-9 expression.** (A-G) *In situ* hybridization of miR-9 on midfrontal E10.5-P15 mouse telencephalic sections. Magnifications of boxed areas are shown below each panel. Scale bars = 400 µm. Abbreviations: cp, cortical plate; e, ependyma; iz, intermediate zone; mz, marginal zone; ppl, preplate; sp, subplate; svz, subventricular zone; vz, ventricular zone; wm, white matter; 2/3/4,5 and 6 are cortical layers.

## 2.2 E14 miR-124 cortical expression patterns in apical and basal compartments

Periventricular neural precursors fall into two distinct compartments, an apical one, self-renewing, including cells with interkinetic nuclear migration and lying entirely within the VZ, and a basal one, derived from the former, including not-motile cells and lying in both VZ and SVZ (Guillemot, 2005; Goetz and Huttner 2005). To finely map previously described different miR-124 expression levels to these compartments, such levels were compared with the distribution of specific protein markers at E14.5. Apical precursors, characterized by high Pax6 expression (Englund et al. 2005), generally displayed faint miR-124 staining (Fig. 10D, box 2). This also specifically applies to a subset of these precursors, the SNPs (Gal et al. 2006) or "pin-like cells" (Ochiai et al. 2009), committed to neuronogenesis and distinguishable, upon E12.5 *in utero* electroporation, thanks to EGFP immunoreactivity driven by the tubulin α1 promoter (Gal et al. 2006) and by retention of process connecting them with the ventricle (Fig. 10G, boxes 1,2).

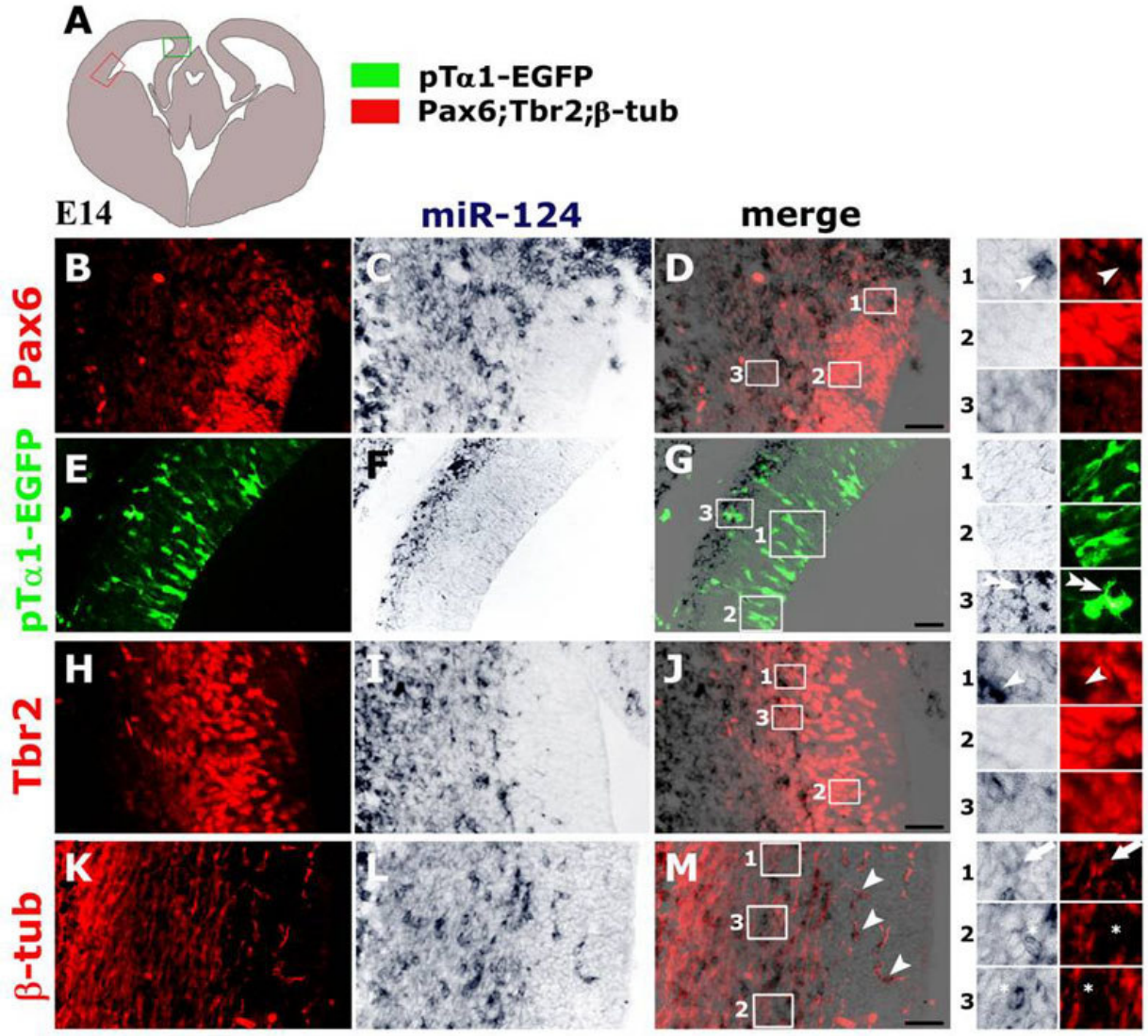


**Figure 10. Comparative profiling of cortical periventricular layers for miR-124 and markers of apical progenitors (Pax6 and pTα1-driven EGFP), basal progenitors (Tbr2) and post-mitotic neurons (β-tubulin).** (A) Schematic of an E14 midfrontal telencephalic section, with the areas subject of analysis. (B,E,H,K) Immunofluorescence of Pax6, pTα1-driven EGFP, Tbr2 and neuron-specific β-tubulin, respectively. (C,F,I,L) *In situ* hybridization of miR-124. (D,G,J,M) Electronic merging of panels (B,E,H,K) and (C,F,I,L), respectively. Numbered magnifications of boxed areas in (D,G,J,M) show Pax6, pTα1-EGFP, Tbr2 and β-tubulin in cells expressing different levels of miR-124 Arrowheads in D1, J1 and M point to Pax6$^{-}$/miR-124$^{high}$, Tbr2$^{-}$/miR-124$^{high}$ and β-tubulin$^{-}$/miR-124$^{high}$ elements, respectively. Double arrowheads in G3 denote pTα1-EGFP$^{+}$/miR-124$^{high}$ cells, not contacting anymore the ventricular cavity. Arrows in M1 indicate SVZ β-tubulin$^{+}$ cells expressing intermediate levels of miR-124. Asterisks in M2,3 demarcate SVZ β-tubulin$^{-}$ cells expressing high levels of miR-124. Scale bars = 100 µm.

Heterogeneous miR-124 expression was conversely detectable in basal precursors, characterized by weak Pax6 staining and robust Tbr2 immunoreactivity (Fig. 10J) (Englund et al 2005). Among Tbr2$^{+}$ cells, presumptively younger elements, lying at more ventricular levels, showed weak miR-124 staining, like apical precursors (Fig. 10J, box 2). On other hand, older elements, lying more marginally (including basal progenitors as well as newborn neurons),

displayed enhanced, intermediate miR-124 staining (Fig. 10J, box 3). Furthermore, isolated Pax6$^-$ and Tbr2$^-$ cells expressed miR-124 at the highest level (Fig. 10D and 10J, arrowheads). Their position correspond to that of VZ and SVZ cells, respectively, co-expressing β-tubulin and abundant miR-124 (Fig. 10M, arrowheads), to be considered as newborn neurons. Remarkably, high miR-124 staining was not tightly restricted to post-mitotic neurons, but could be detected also in some β-tubulin$^-$ elements within the SVZ (Fig. 10M, asterisks), to considered as basal progenitors (Haubensak et al. 2004). On the other hand, again in the outer SVZ, not all β-tubulin$^+$ neurons expressed miR-124 at the highest levels (Fig. 10M, arrows), suggesting a relevant variability in miR-124 up-regulation along the neuronogenic lineage.

### 2.3 *in vitro* and *in vivo* overexpression of miR-124

To cast light on the role played by miR-124, we developed a set of molecular tools for gain-of-function analysis. We cloned the Pri-miR-124(2) cDNA fragment (Griffiths-Jones et al. 2006, Grimson et al., 2006) into the BLOCK-iT™ expression vector (Invitrogen), in-between the pCMV/EmGFP and the TKpA modules, in place of Pri-miR-155 derivative cDNA sequences (plasmid pPri-miR-124(2)). BLOCK-iT was kept as negative control expression vector (pPri-miR-155neg_control). To assess the effectiveness of pPri-miR-124(2) to over-express mature miR-124, we built up a dedicated sensor plasmid, cloning a Lhx2_3'UTR cDNA fragment harboring two miR-124 responsive elements (Griffiths-Jones et al. 2006, Krek et al, 2005), into the pDsRed2-N1 plasmid (Clontech), in-between the pCMV/DsRed2 and the SV40pA modules (plasmid pmiR-124-sensor) (Fig. 11A). Compared with pPri-miR-155neg_control/pmiR-124-sensor control, cotransfection of pPri-miR-124(2) and pmiR-124-sensor on Hela cells specifically reduced the fraction of fluorescent cells expressing DsRed2, by about 60% (Fig. 11B, C). To overexpress miR-124 in primary cortical precursor cells, we transferred the Pri-miR-124(2) cDNA fragment into the DsRed2-derivative of the constitutive lentiviral expressor pCCLsin.PPT.prom.EGFP.Wpre (Follenzi and Naldini, 2002). Transduction of primary cortical precursor cells with the resulting LV_Pri-miR-124(2) promoted neuronal generation, as shown by the increase of β-tubulin expressing cells at 72 hours post-infection (PI) (Fig. 11F,G). Enhancement of neuronal differentiation induced by LV_Pri-miR-124(2) was further confirmed by the increase of average total neurite length, calculated at 72 hours PI on low density cultures by NeuriteTracer® (Fig. 11H,I) (Pool et al, 2008). Such effects took place specifically under

2,5% fetal calf serum (FCS) (Fig. 11F-K). *In vivo* electroporation of pPri-miR-124(2) into E12.5 lateral cortex resulted in specific up-regulation of miR-124 in periventricular layers (Fig. 11J,K).

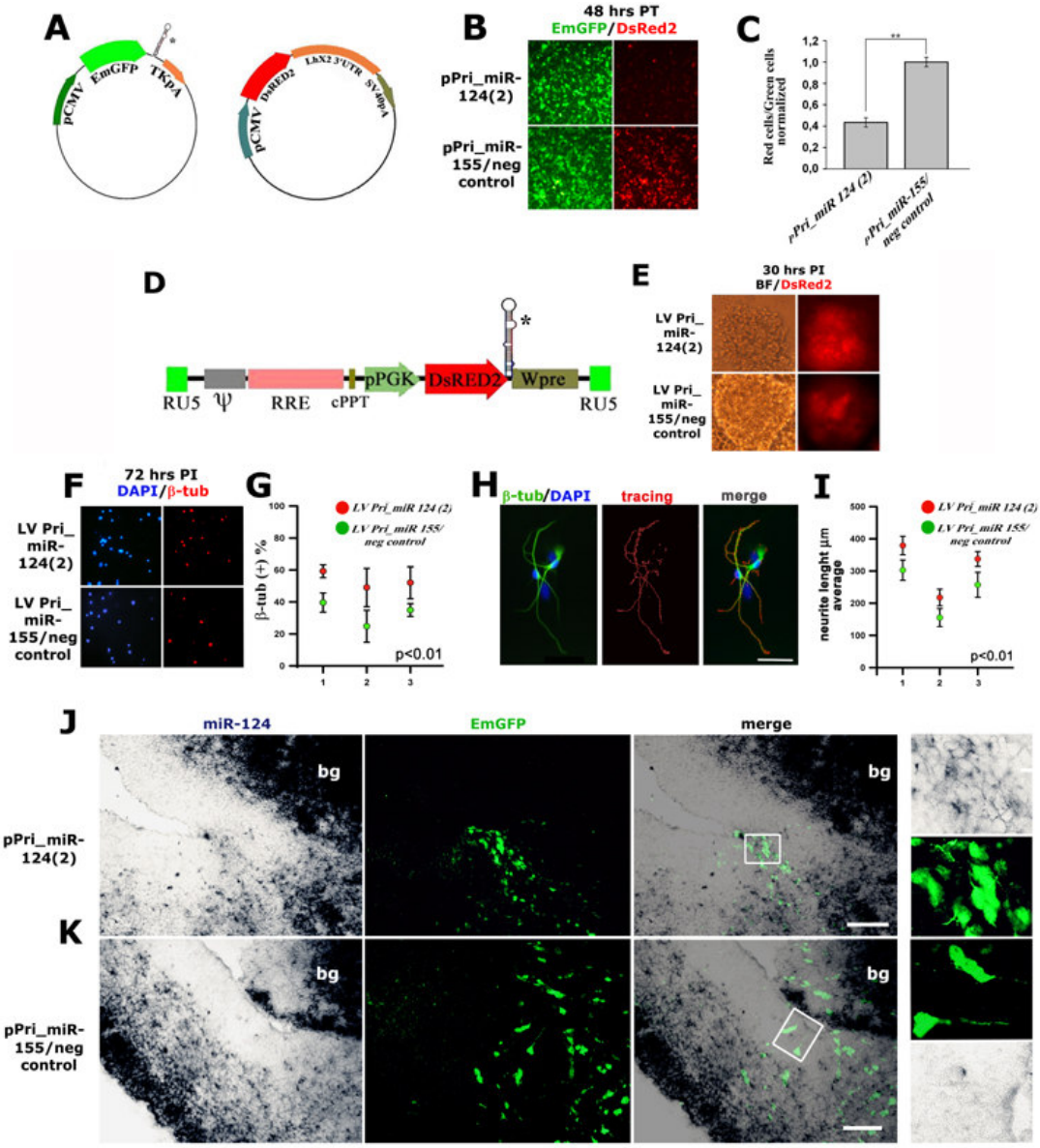


**Figure 11. Overexpressing miR-124 *in vitro* and *in vivo*.** (A) Backbone of the expression plasmids pPri-miR-124(2)/155/neg_control; miR-124-responsive sensor plasmid pCMV/DsRed2/*Lhx2*_3'UTR. The asterisk indicates the position of Pri-miR cDNA fragments. (B,C) Specific attenuation of DsRed2 expression in Hela cells cotransfected with pPri-miR-124(2) and pCMV/DsRed2/*Lhx2*_3'UTR. (D) Backbone of lentivectors LV_Pri-miR-124(2)/ 155/neg_control. The asterisk indicates the position of Pri-miR cDNA fragments. (E) DsRed2 expression in E12.5 primary cortico-cerebral progenitors, infected by lentiviruses LV_Pri-miR-124(2)/ 155/neg_control, at MOI = 40, and kept for 30 hours under 2,5% serum-added DMEM:F12:N2 medium. (F,G) Differential β-tubulin immunoprofiling of acutely dissociated, E12.5 infected cortical progenitor cells at 72 hours PI. (H) Example of neurite outgrowth evaluation by immunostaining and subsequent NeuriteTracer® analysis. (I) Differential neurite outgrowth in low density E12.5 infected cortical progenitor cells at 72 hours PI, calculated in 3 different experiments by NeuriteTracer®. (J,K) *In vivo* overexpression of miR-124 in lateral neocortex. Distribution of miR-124 and pCMV-driven-EmGFP on E14.5 midfrontal telencephalic sections, from brains electroporated at E12.5 with the plasmids pPri-miR-124(2)/155/neg_control, respectively. Magnifications of boxed insets of electronic merges are shown to the right. Abbreviations: bg, basal ganglia. In (C): error bars represent the s.e.m. calculated among the means of each experiment; double asterisk means $p<0.01$, as evaluated by ANOVA test; N=3,3. In (G,I): error bars represent the s.e.m. calculated within each experiment; the $p<0.01$ value was evaluated by t-test (1-tail, paired); N=3,3. Scale bars = 40 µm (H) and 100 µm (I).

However, at a more detailed analysis, the amplitude of such up-regulation was moderate and only strongly electroporated periventricular cells expressed miR-124 at levels above the local natural range (Fig. 11 and data not shown). This might depend on poor processing of Pri-miRs sequences to mature miRNAs, peculiar to undifferentiated cells (Thomson et al, 2006; Wulczyn et al. 2007; Obernosterer et al. 2006). Consistently with this hypothesis, neuroblasts infected by LV_Pri-miR-124(2) and allowed to differentiate under FCS, specifically and progressively down-regulated DsRed2 (Fig. 12), compatibly with an enhanced maturation of their primary DsRed2/miR-124(2) transcripts to Pre-miR-124.

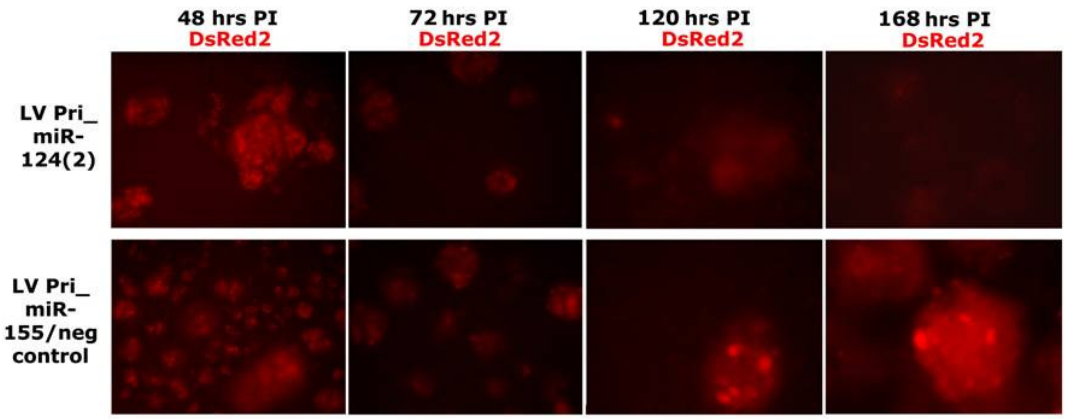


**Figure 12**. Time-course DsRed2 fluorescence in primary cortical precursors cultures infected by Pri-miR expressing lentiviruses. Divergent temporal progression of DsRed2 fluorescence in E12.5 neuroblasts infected by LV_Pri-miR 124(2) or LV_Pri-miR-155/neg_control and allowed to differentiate under FCS. Abbreviations: PI, post-infection.

## 2.4 Periventricular expression of Pri/Pre-mir-124(2) at embryonic stage E14.5

To cast-light on the hypothesis of a posttranscriptional modulation of the Pri-miR-124 sequences in neural precursors, we designed a 24 bp LNA probe (Exiqon®) against the loop region of Pri/Pre-miR-124(2) (fig. 13E). *In situ hybridization* of such sequence on E14.5 mice coronal slices gave rise to a signal throughout the cortex, with reinforcement in the cortical plate (fig. 13A-C). Pre-miR-124 labeled cells were tightly restricted to the CNS and were completely absent in the surrounding mesenchymal tissue, ruling out the possibility of a signal due to any background of the designed probe (fig. 13E,F). The robust staining in VZ cells confirms the hypothesis that regulation of miR-124 levels includes a modulation of Pri/Pre-miR-124(2) maturation in dividing neural precursors, similar to what previously described for different microRNAs in stem cells (Wulczyn et al, 2006; Obernosterer et al, 2006). Nevertheless, the

higher signal of unprocessed Pre-miR-124(2) in postmitotic cells of the cortical plate also suggests a concurrent modulation of miR-124 expression at transcriptional level, as previously described in different reports (Conaco et al, 2006; Makeyev et al, 2007)

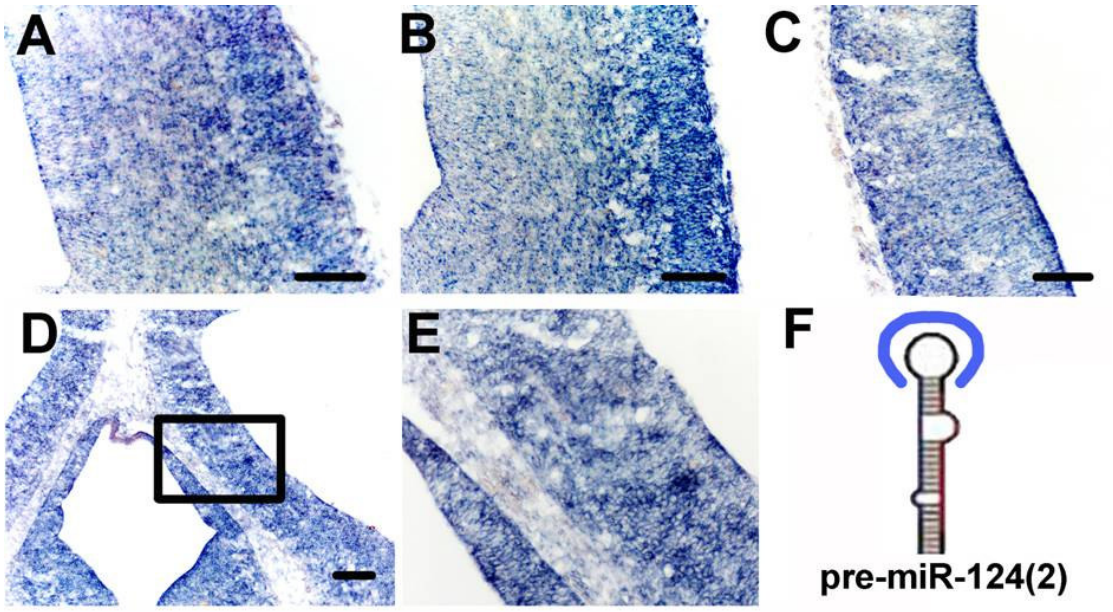


**Figure 13**. **Expression of miR-124 precursor in VZ/SVZ periventricular layers at E14.5.** *In situ* hybridization of the Pri/Pre-miR-124(2) on E14.5 mouse telencephalic sections. Lateral neocortex (A,B) and archicortex (C,D) of four different embryos. (E) Boxed area in D illustrates only a slight signal in some cells of mesenchymal tissue probably due to technical background. (F) Schematic of the designed probe used for Pri/Pre-miR-124(2) *in situ* hybridization. Scale bar= 100 µm.

Further investigations are necessary to finely describe in VZ dividing cells at which level of microRNAs processing such posttranscriptional modulation take place and if such process is common to all three miR-124 genes.

### 2.5 *In vivo* promotion of neuronogenesis by miR-124

The miR-124 expression pattern reported above suggested us an active involvement of this miRNA in promotion of cortico-cerebral neuronogenesis. To confirm this prediction and to clarify cellular mechanisms underlying such promotion, we electroporated pPri-miR-124(2) or pPri-miR-155neg_control into the lateral ventricle of E12.5 mouse embryos and, two days later, immunoprofiled EmGFP$^+$ electroporated cells and their progenies for molecular markers of neural precursors and newborn neurons. Per each marker, at least 3+3 embryos (N≥3,3), electroporated with either pPri-miR-124(2) or pPri-miR-155neg_control constructs, were analyzed and, per every embryo, at least 400 EmGFP$^+$ cells were scored. Upon pPri-miR-124(2) electroporation, the fraction of intermitotic EmGFP$^+$ cells was specifically reduced by 20% (N=5,5; $p<0.05$), when assessed by the S-phase marker terminally-administered-BrdU. However,

it did not display any statistically relevant change, if evaluated by the M-phase marker phospho-histone3 (PHH3) (N=3,3). EmGFP$^+$ cells expressing the apical precursor marker Pax6 decreased by 20% (N=4,4; $p<0.05$) and, conversely, those positive for the basal precursor marker Tbr2 increased by a similar percentage (Fig. 14) (N=5,5; $p<0.05$).

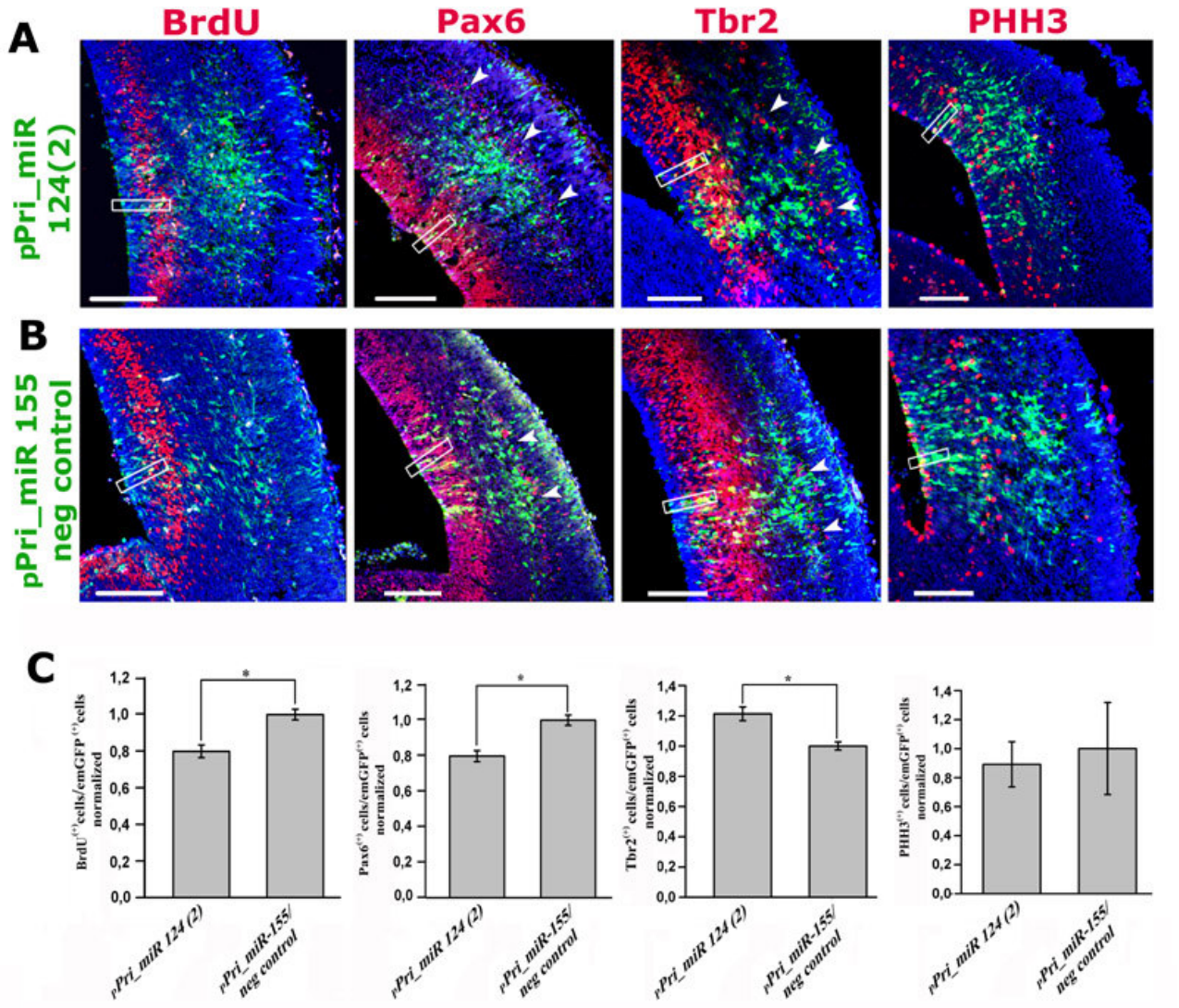


**Figure 14. Immunoprofiling of cortical periventricular layers upon *in utero* electroporation of plasmids pPri-miR-124(2) and pPri-miR-155/neg_control (I).** (A,B) Distribution of terminally administered BrdU, Pax6, Tbr2, PHH3 and pCMV-driven EmGFP on E14.5 mid-frontal sections, from brains electroporated *in utero* at E12.5 with plasmids pPri-miR-124(2) and pPri-miR-155/neg_control. Arrowheads point to abventricular displaced cells expressing Pax6 and Tbr2. Insets illustrate examples of EGFP/marker co-localizations, subject of counting and statistical analysis. (C) Fractions of EmGFP$^+$ cells immunoreactive for BrdU, Pax6, Tbr2 and PHH3. Simple asterisk, $p<0.05$, as calculated by ANOVA test; N=5,5 for BdU and Tbr2; N=4,4 Pax6; N=3,3 for PHH3. Scale bars = 100 µm

Electroporation of both pPri-miR-124(2) and pPri-miR-155neg_control also led to displacement of apical Pax6$^+$ and of basal Tbr2$^+$ precursors towards the cortical plate (in 6 out of 8 embryos and in 8 out of 10 embryos, respectively) (Fig. 14A, B, arrowheads). This

phenomenon was not restricted to electroporated cells, but mainly interested their *close* surroundings. Since the two plasmids shared a similar stem-and-loop Pri-miR moiety, to assess if such displacement were specifically linked to over-expression of this structure, we performed a further electroporation with the control plasmid pEGFP-C1™ (Clontech), harboring the same pCMV/GFP module but missing the Pri-miR element. Remarkably, even in this case, Pax6 and Tbr2 displacements were evident (both in 3 out of 3 electroporated embryos), so ruling out they were due to the Pri-miR moiety and indicating they were consequence of the *in utero* electroporation protocol followed (Fig. 15, arrowheads).

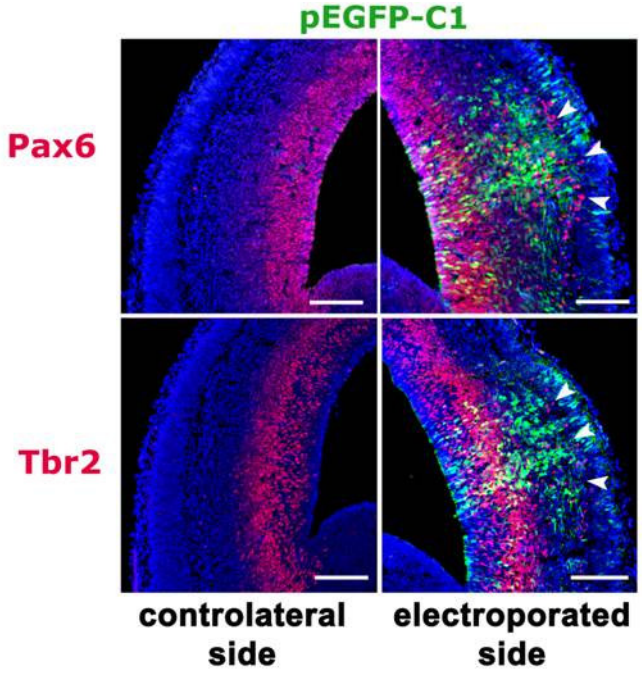


**Figure 15. Displacement of apical, Pax6$^+$, and basal, Tbr2$^+$, precursors within the cortical wall of E14.5 brains, electroporated two days earlier with pEGFP-C1.** Arrowheads point to abventricularly displaced Pax6$^+$ and Tbr2$^+$ elements, both positive and negative for electroporated EGFP. Such displaced cells were not detectable in the controlateral, not electroporated side of same embryos (N=3). Scale bar = 100 µm

In 2 out of 5 analyzed embryos, pPri-miR-124(2) electroporation specifically elicited strong activation of post-mitotic markers β-tubulin (Fig. 16A, B, arrowheads) and Tbr1 (Englund et al, 2005) (Fig. 16D, E, arrowheads) as well as neurite outgrowth (Fig. 17, arrowheads) in the VZ. These effects were associated to strong over-expression of miR-124 in this zone (Fig. 16C, arrows). In a few words, overexpression of miR-124 seems to promote precursors transition from the apical to the basal compartment and to stimulate direct differentiation of apical progenitors to post-mitotic neurons.

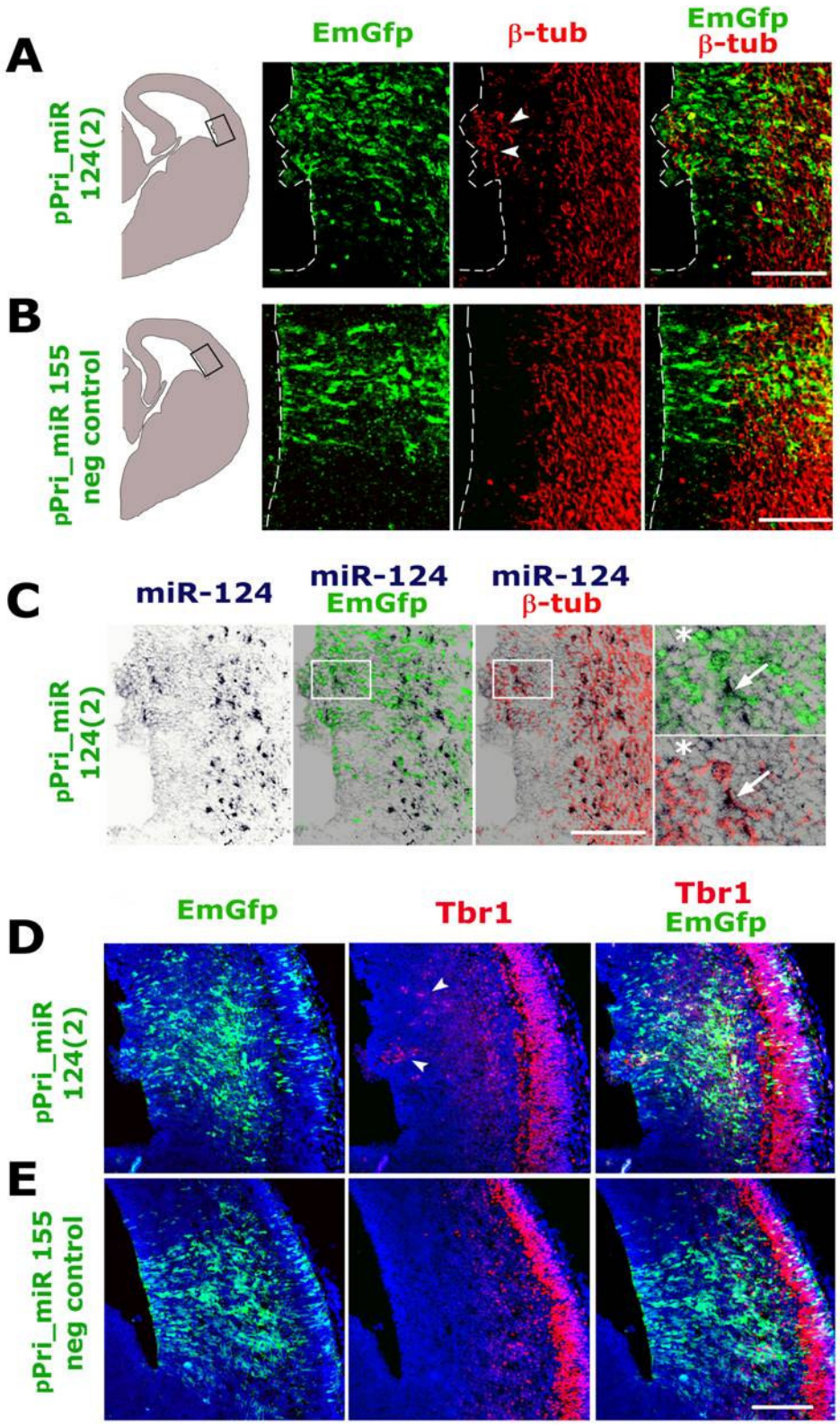


**Figure 16. Immunoprofiling of cortical periventricular layers upon *in utero* electroporation of plasmids pPri-miR-124(2) and pPri-miR-155/neg_control (II).** (A,B,D,E) Distribution of β-tubulin, Tbr1 and pCMV-driven EmGFP on E14.5 mid-frontal sections, from brains electroporated *in utero* at E12.5 with plasmids pPri-miR-124(2) -155/neg_control. In (A) and (D), arrowheads point to periventricular cells expressing β-tubulin and Tbr1, respectively. (C) Comparison of pCMV-driven EmGFP and neuron-specific β-tubulin with miR-124 expression in the electroporated area shown in (A,B,D,E). Magnifications of boxed insets to the right show an $EmGFP^+$ electroporated cell co-expressing huge amounts of miR-124 and β-tubulin (arrow), as well as another $EmGFP^+$/$miR\text{-}124^+$ cell negative for β-tubulin (asterisk). Scale bars = 100 μm

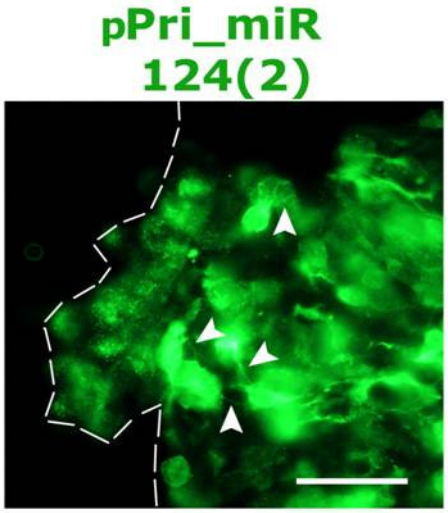


**Figure 17. VZ neuronal differentiation in E14.5 cerebral cortex, electroporated two days earlier with pPri-miR-124(2).** Arrowheads show outgrowing neurites within the VZ. Scale bar = 10 µm.

As suggested by activated-Caspase3 immunoprofiling of electroporated tissues (N=4,4), the shifts described above seems not to arise as a consequence of differential cell death (Fig. 18). Finally, high-level miR-124 expression elicited in *apical* progenitors (including pin-like cells; Fig. 19, arrowheads) upon *in vivo* electroporation may support these phenomena.

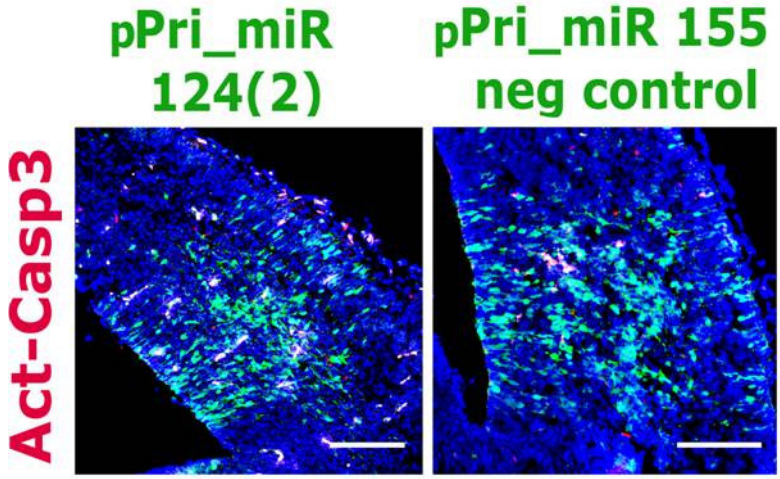


**Figure 18. Distribution of activated-Caspase3$^{+}$.** Apoptotic cells within the cortical wall of E14.5 brains, electroporated two days earlier with pPri-miR-124(2) or pPri-miR-155/neg_control (N=4,4). Scale bar = 100 µm

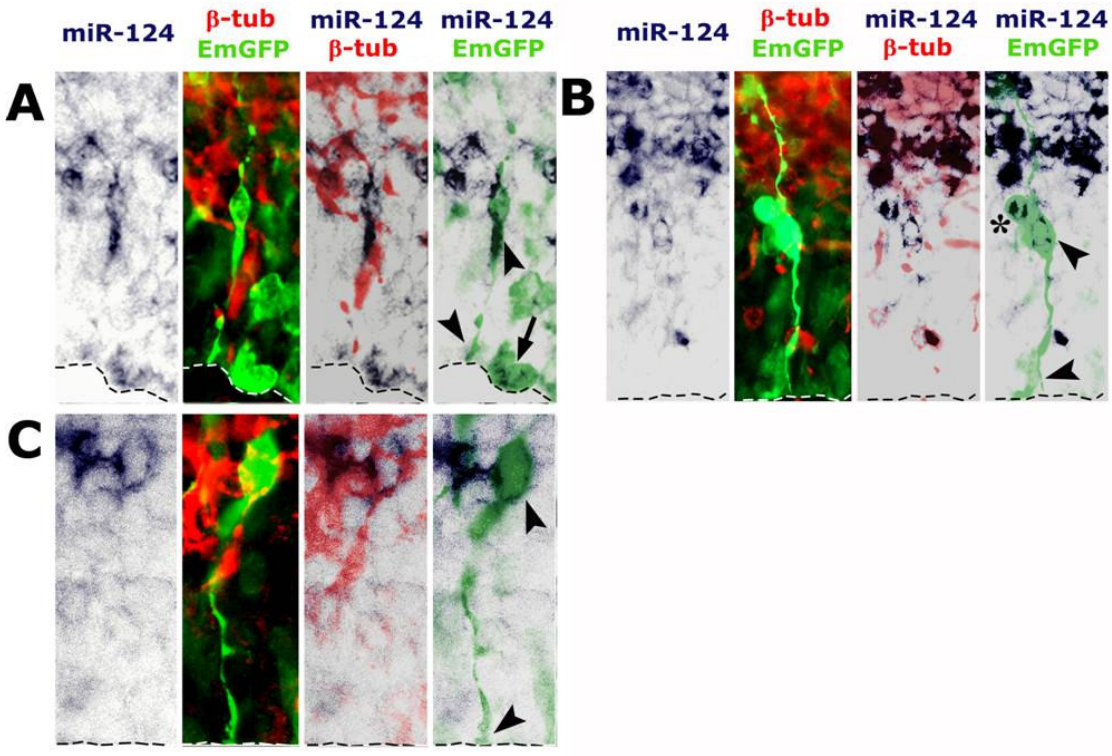


**Figure 19. Specific miR-124 overexpression in pPri-miR-124(2) electroporated periventricular neural precursors of the E14.5 cortex**. Distribution of miR-124, pCMV-driven EmGFP and neuron-specific β-tubulin on mid-frontal sections, from brains electroporated in utero at E12.5 with pPri-miR-124(2). miR-124 may be specifically detected in: apical progenitors still connected to the ventricle (arrowheads in (A) and (B)) or undergoing mitosis (arrow in (A)); basal progenitors (asterisk in (B)); nascent neurons still connected to the ventricle (arrowheads in (C)).

Looking for mechanisms linking miR-124 overexpression with promotion of apical-to-basal transition, we assayed expression of β1-integrin. This protein is necessary for integrity of adherens junctions among radial glial cells and the subpial basal membrane (Graus-Porta et al, 2001) and is an established target of miR-124 in the chicken (Cao et al, 2007). The cortical expression profile of β1-integrin normally included a strong signal in VZ, transitional field (TF) and MZ and a palisade-like pattern in the CP, possibly corresponding to pial processes of radial glia and migrating neurons, over-imposed to a weaker signal of resident neurons (Fig. 20). This is a domain quite complementary to that expressing miR-124 at high level. Unexpectedly, however, electroporation of Pri-miR-124(2) in the mouse cerebral cortex did not elicit any detectable down-regulation of β1-integrin. This may mean that miR-124-dependent regulation of β1-integrin, peculiar to the chicken neural tube, does not take place in the mammalian cortex. Alternatively, this may be due to poor sensitivity of our immunodetection technique in discerning subtle changes in antigen concentration

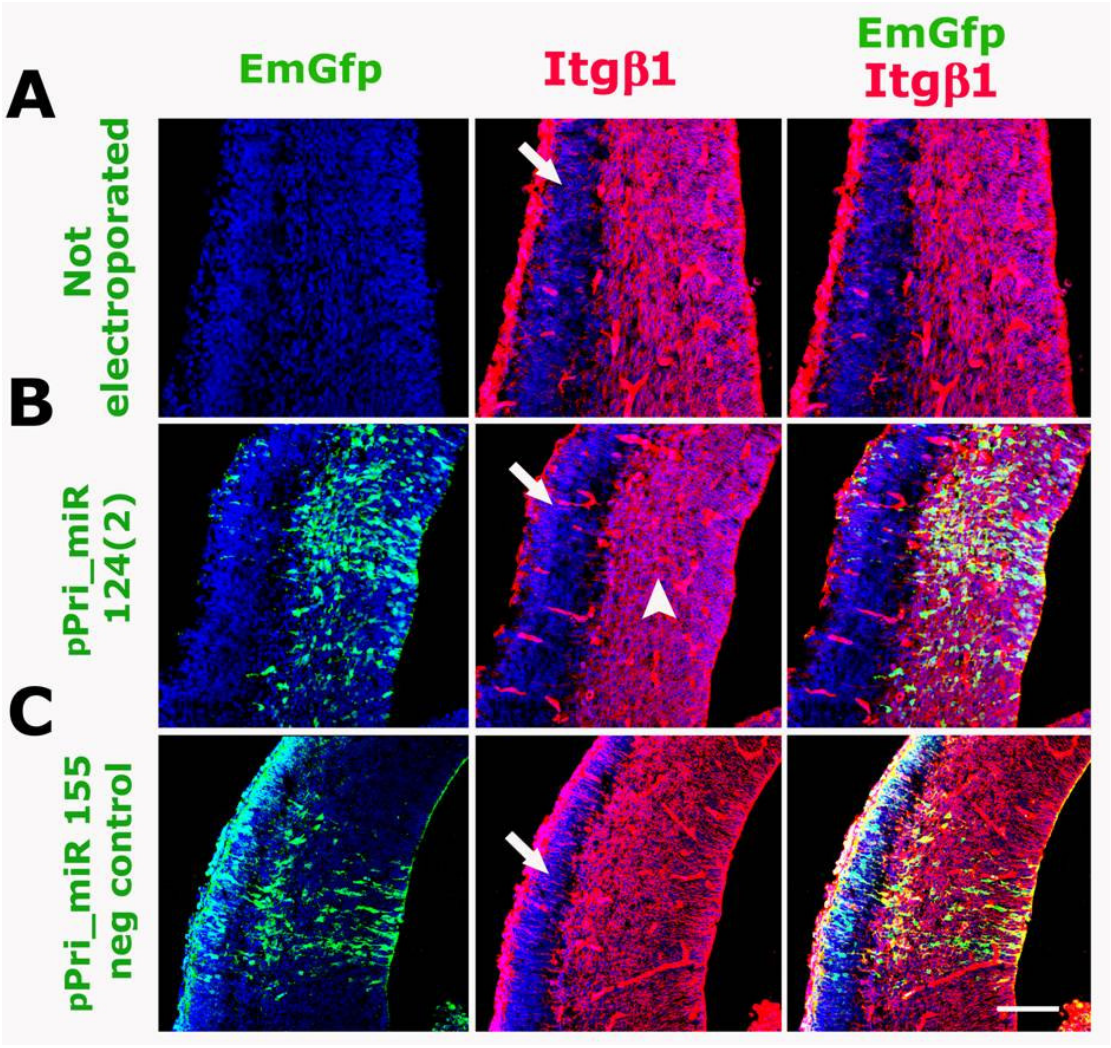


**Figure 20. Distribution of β1-integrin within the cortical wall of E14.5 brains, electroporated two days earlier with pPri-miR-124(2) or pPri-miR-155/neg_control.** The arrowhead in B points to the pPri-miR-124(2)-electroporated region, not displaying any overt reduction of β1-integrin immunoreactivity. Arrows in (A-C) denote the cortical plate, where β1-integrin is down-regulated and restricted to radial glial fibers. Scale bar = 100 μm

# 3. Discussion

In this study, by integrating LNA-oligo *in situ* hybridization, electroporation of stage-specific reporters and immunofluorescence, we carefully reconstructed the miR-124 expression pattern in the developing mouse cerebral cortex. Moreover, by *in vitro* lentivirus-based gene transfer and *in utero* electroporation of gain-of-function plasmids, we investigated activities played by this molecule in the embryonic neuronogenic process.

We confirmed that miR-124 is progressively up-regulated during the embryonic neuronogenesis, as previously reported (De Pietri-Tonelli et al, 2006; Deo et al, 2007; Makeyev et al, 2008; Cheng et al, 2009). In particular, with the appearance of the SVZ, we found that miR-124 displayed three distinct expression levels, low in the VZ (Cheng et al, 2009, De Pietri-Tonelli et al, 2006), intermediate in the SVZ and high in more marginal layers (Fig. 7 and 8). The presence of isolated β-tubulin$^+$ cells and Pax6$^-$ cells within the VZ, both highly expressing miR-124, suggested us that an abrupt upregulation of miR-124 might occur during direct neuronogenesis (Fig. 10 and 21A). The miR-124 expression profile appeared conversely biphasic in indirect neuronogenesis. Here, a low-to-middle expression transition took place within Tbr2$^+$ basal progenitors, having lost contact with the ventricular cavity, and a further upregulation could be alternatively localized in basal progenitors or early post-mitotic β-tubulin$^+$ neurons (Fig. 10 and 21B). This scenario is reminiscent of what was found by Doetsch and coll. in the adult SVZ (Cheng et al, 2009). Here a former upregulation of miR-124 occurs after the neural stem cell-to-transit amplifying cell transition and a further upregulation is approximately associated to the exit of neuroblasts from cell cycle (Deo et al, 2007, Cheng et al, 2009). Finally, we specifically detected an accumulation of cells highly expressing miR-124 and with multipolar morphology at the border between VZ and SVZ, from E14.5 onward (Fig.7 and fig.10I,L). Such accumulation recalls the “sojourn band” or “multipolar accumulation zone” (MAZ), where newborn neurons settle before initiating their radial migration (Bayer and Altmann, 1991; Noctor et al, 2004; Tabata et al, 2009).

Electroporation of our gain-of-function constructs was followed by concerted up-regulation of EmGFP and miR-124. Such up-regulation was relatively weak for miR-124; however, levels of this miRNA in electroporated apical precursors often emerged above endogenous VZ expression levels, so allowing functional perturbation of the system (Fig. 11 and 19). Limited production of miR-124 despite of abundant EmGFP/Pri-miR-124(2) transcript available in apical progenitors might stem from sub-optimal, regulated processing of this chimeric transcript to mature miRNA. This hypothesis is consistent with the discrepancy among expression profiles of

miR-124, mainly restricted to abventricular layers (Fig. 7 and 10), and of its precursors, conversely detectable - at E14.5 - at similar levels throughout the cortical wall (fig. 13; Deo et al, 2007). This may also account for progressive lowering of DsRed2 fluorescence we found in *in vitro* differentiating neurons, harboring a DsRed2/Pri-miR-124(2) transgene. The idea that a substantial modulation of miRNA levels may occur after transcription is not novel. In addition to transcriptional regulation (Conaco et al, 2006; Zhao et al, 2005), it has been suggested and experimentally proven that biogenesis of many miRNAs may be regulated at a variety of levels, including Drosha-dependent Pri-miR-to-Pre-miR conversion (Davis et al, 2008), nucleo-to-cytoplasm Pre-miR translocation (Lund et al, 2004), Dicer-dependent Pre-miR-to-miR conversion (Obernosterer et al, 2006), miRNAs incorporation into RISC (Hwang et al, 2009). Modulation of Pri-miRs processing is especially relevant to proper regulation of neuro-specific and neuro-enriched miRNAs, including *let-7* family members, *miR-128* and *miR-138*, whose post-transcriptional maturation may dramatically increase with the transition from stem cells to post-mitotic differentiated elements (Thomson et al, 2006; Wulczyn et al, 2007; Obernosterer et al, 2006). Preferential confinement of many miRNAs precursors maturation to late histogenesis is consistent with the integrity of stem cells within the cortical VZ of *Dicer* conditional-null mutants (Makeyev et al, 2007; De Pietri-Tonelli et al, 2008), as well as with the impaired differentiation abilities of *Dicer*$^{-/-}$ ES cells (Kanellopoulou et al, 2005). Post-transcriptional regulation of miR-124 has been already addressed in the developing *Drosophila* nervous system, where dFMR1 is required for its proper biogenesis (Xu et al, 2008). Further studies have to be run in order to clarify modulation of miR-124 expression in vertebrates.

By electroporating a Pri-miR-124(2) precursor into the developing mouse cortex, we were able to promote cortical neuronogenesis. We forced a fraction of ventricular precursors to leave the apical compartment and to move to the basal compartment (Fig. 14). We occasionally anticipated β-tubulin activation in pin-like cells (Fig. 19C) and elicited an ectopic burst of neuronogenesis from apical progenitors within the ventricular zone (Fig. 16 and 17). We replicated the last result *in vitro*, by over-expressing Pri-miR-124(2) in dissociated cortical neuroblasts, but only when these precursors were kept under differentiating medium (Fig. 11F-I). Inhibition of BrdU uptake and stimulation of direct neuronogenesis has been already reported in the chicken embryonic spinal cord, specifically upon electroporation of mature miR-124 (Visvanathan et al, 2007; Cao et al, 2007). A reduction of dividing cells also takes place *in vivo,* in the adult mouse SVZ, upon Pri-miR-124(3) overexpression. Consistently, administration of antisense miR-124 to *in vitro* cultures of SVZ elements increases BrdU uptake by C-type transit amplifying cells and A-type neuroblasts, slowing down transition from the former to the latter

ones (Cheng et al, 2009). Remarkably, we also found that miR-124 facilitates neuronogenesis in a permissive molecular environment, but is not able to initiate such a process *per se*, similar to what previously described (Krichevsky et al, 2006; Makeyev et al, 2007; Yu et al, 2008). Finally, we did not find any increase of cell death upon Pri-miR-124(2) electroporation (Fig. 18), differently from what previously reported in the chicken embryo (Cao et al, 2007). This may originate from a variety of reasons, including differences among animal models, distinct CNS tracts subject of analysis, constructs and electroporation protocols.

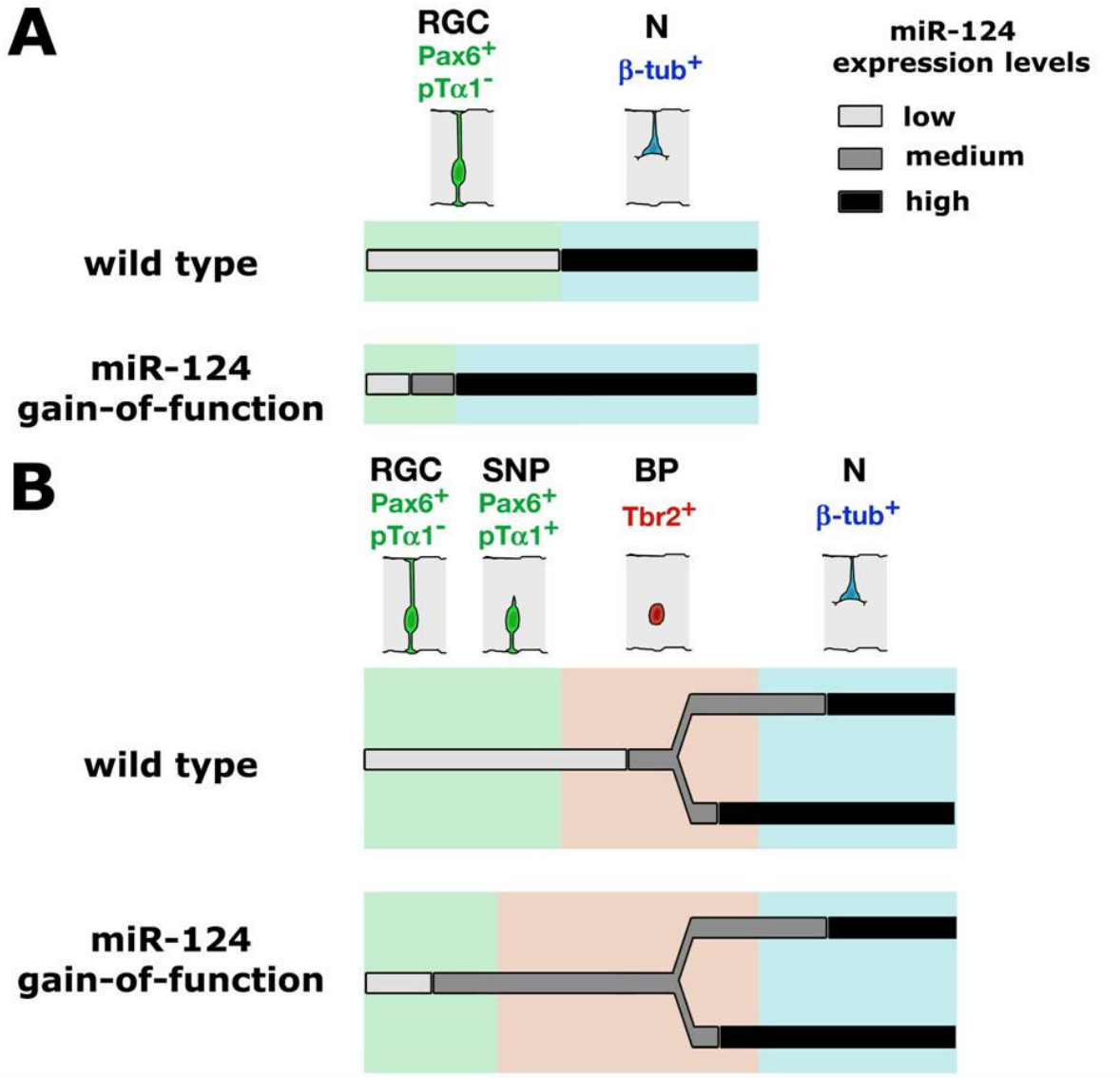


**Figure 21. Schematic of the miR-124 expression profile along neuronogenic lineages and phenotype of miR-124 gain-of-function electroporated cortices.** One-step and two-steps changes of miR-124 expression levels during direct (A) and indirect (B) neuronogenesis, respectively. Stimulation of direct neuronogenesis and expansion of the basal compartment at expenses of the apical one, upon miR-124 over-expression.

At the end, by analyzing electroporated brains, we noticed a previously undescribed technical artifact. We detected a pronounced displacement of apical $Pax6^+$ and basal $Tbr2^+$ progenitors, just beneath the cortical plate, in both pPri-miR-124(2) and pPri-miR-155_neg_control electroporated brains (Fig. 14, arrowheads). This phenomenon was replicated upon electroporation of pEGFP-C1 (Fig. 15, arrowheads), which shares the pCMV-EGFP module with the previous two plasmids but does not harbor the Pri-miR stem-and-loop moiety, so ruling out any miR-124- or stem-and-loop specificity of its origin. Displacement of apical and basal precursors took place only on the electroporated side, was mainly restricted to the middle of the electroporated zone, being not detectable in its surroundings, and was not cell-autonomous (Fig. 15). Despite of the locality of such displacement, the electric field we applied was uniform throughout the E12.5 telencephalon, thanks to the 7mm tweezer electrodes we used. This implies that such effect was not due to the electrical stress *per se*. Reasonably, it might originate from heavy metabolic loads weighing on electroporated precursors, possibly impairing the correct scaffold structure of the cortical wall. The mechanical damage induced by the injection needle might contribute to the priming of such effect. Nevertheless, displacement of $Pax6^+$ and $Tbr2^+$ progenitors was equally present in controls and Pri-miR-124(2) electroporated embryos, so not affecting the results of miR-124 gain-of-function analysis.

# 4. Methods

## 4.1 Animals and bromodeoxyuridine (BrdU) injection

Mice (*Mus musculus*, strain CD1 purchased from Harlan-Italy) were maintained at the SISSA-CBM mouse facility and were staged by timed breeding and vaginal plug inspection. Animals handling and subsequent procedures were in accordance with European laws [European Communities Council Directive of November 24, 1986 (86/609/EEC)] and with National Institutes of Health guidelines. Embryos (E10.5-E18.5) were harvested from pregnant dames killed by cervical dislocation. When required, BrdU was injected intraperitoneally into previously electroporated pregnant dams 45 minutes before the sacrifice, at 150 µg/g bodyweight. Straight after electroporated embryos were harvested.

## 4.2 Pri-miRNA and cDNA expression contructs

The pPri-miR-124(2) construct contains the 285-bp mouse Pri-miR-124(2) genomic fragment (chr3 (+):17695562-17695846) cloned into the BLOCK-iT™ expression vector (Invitrogen), in-between pCMV-EmGFP and TK_pA modules, using *SalI* and *XbaI* enzyme restriction sites. The pPri-miR-155neg_control contains the Pri-miR155 sequence in-between pCMV-EmGFP and TK_pA modules (BLOCK-iT™, Invitrogen). The plasmid pmiR-124-sensor contains the 477-bp 3'UTR fragment of mouse *Lhx2* (chr2 (+):38224759-38225235) cloned into the pDsRed2-N1 plasmid (Clontech), in-between the pCMV/DsRed2 and the SV40pA modules, using *NotI* and *EcoRV* enzyme restriction sites. pTα1-EGFP plasmid (a kind gift by E. Ruthazer) harbors the GFP cds under the control of the β-tubulin 1 promoter (pTα1). pLV_Pri-miR-124(2) and pLV_Pri-miR-155neg_control, encoding for lentiviral RNA genomes, were generated as follows. Briefly, the Pri-miR-124(2) and Pri-miR-155neg_control *DraI-BglII* fragments were transferred from pPri-miR-124(2) and pPri-miR-155neg_control, respectively, into the pDsRed2-N1 *NotI_blunted-BglII* cut plasmid, downstream the DsRed2 module. Subsequently, the DsRed2-Pri-miR-124(2) and the Dsred2-Pri-miR-155neg_control *AgeI-SmaI* fragments were transferred from the resulting plasmids into the pCCLsin.PPT.prom.EGFP.Wpre [49] *AgeI-SalI_blunted* cut vector. pEGFP-C1 (Clontech) was used as control for *in utero* electroporation.

## 4.3 Production and titration of lentiviral vectors

Plasmids pLV_ Pri-miR-124(2) and pLV_ Pri-miR-155neg_control were used to produce lentiviral vectors LV_ Pri-miR-124(2) and LV_ Pri-miR-155neg_control as previously described

(Follenzi and Naldini, 2002). Titration of lentiviral vectors was performed by Real-Time PCR on extracted Dna, as previously reported (Sastry et al, 2002).

### 4.4 miR-activity assay

HeLa cells, grown in 10% Fetal Calf Serum (FCS) Dulbecco's modified Eagle's medium with Glutamax (DMEM/Glutamax-Invitrogen™), were co-transfected with either pPri-miR-124(2) or pPri-miR-155neg_control, each pre-mixed with pmiR-124-sensor plasmid at a molar ratio of 30:1, using Lipofectamine (Invitrogen™) and according to Manifacturer's instructions. 48 hours after transfection, photos of 10 different, randomly chosen fields of each plate were taken, using a Nikon Eclipse 80i fluorescent microscope (20X lens) and a DS-2MBWC digital microscope camera. Pictures were processed by Photoshop CS3 software and specific attenuation of DsRed2 signal was evaluated by comparing the numbers of single and doubles labeled cells. All cell countings were performed on coded samples, so that the experimenter was blind to the condition. The experiment was repeated three times and data analyzed using Excel 2008™ and SigmaPlot™.

### 4.5 Lentiviral gene transduction on differentiating primary cortical precursor cells.

To evaluate the fraction of beta-tubulin$^+$ cells among differentiating primary cortical precursor cells, cerebral cortices of E12.5 embryonic brains were dissected as previously described [68]. $3*10^6$ cells were plated onto each well of a 12-multiwell plate (Falcon™), at a density of $10^3$cells/microliter and cultured in DMEM/F12/Glutamax medium (Invitrogen™), integrated with N2 supplement (Invitrogen™), 0.6% w/v glucose, 2 µg/ml heparin, 10 pg/ml fungizone, with or without 2.5% fetal calf serum (FCS). Cortical precursors were transduced with lentiviral vectors at a multiplicity of infection (MOI) of 40. Medium was replaced 36 hours post-transduction. For the experiments of neurite outgrowth, $5*10^5$ cells were plated onto each well of a polylysined 12-multiwell plate (Falcon™), at a density of 200 cells/microliter and cultured as above. This lower density culture was necessary to allow for subsequent NeuriteTracer® analysis of differentiating cells.

### 4.6 Evaluation of neuronal frequencies in vitro

72 hours after lentiviral infection, *in vitro* transduced cells were dissociated with trypsin-EDTA for 5 minutes, left to attach on poly-L-lysine coated glass coverslips for 30 minutes and finally fixed by 4% paraformaldehyde. Staining was performed as previously described (Gritti et al, 1996) with primary mouse monoclonal antibody anti-β-tubulin (clone Tuj1, Covance, 1:300) and

anti-mouse secondary antibody Alexa fluor 594 conjugates (Invitrogen™; 1:500). DAPI (4', 6'-diamidino-2-phenylindole) was used as nuclear counterstaining. For each experiment 5+5 fields were captured using a fluorescent Nikon Eclipse 80i microscope (20X lens) and a DS-2MBWC digital microscope camera. For each experiment, at least 300+300 cells were counted. The experiment was repeated three times; data were analyzed as follows. Frequencies of β-tubulin+ cells within each field were calculated. They were averaged per each experiment and each lentivirus therefore the results (± s.e.m.) plotted against experiment numbers. Finally, the so-obtained 3+3 average frequencies were analyzed by t-test (1-way, paired) and the p-value reported on the graph.

### 4.7 Evaluation of in vitro neurite outgrowth

72 hours after lentiviral infection, *in vitro* transduced cells were fixed for 15 minutes by 4% paraformaldehyde. β-tubulin/DAPI staining was performed as described in Cells immunofluorescence, replacing the Alexa fluor 594 antibody with Alexa fluor 488. For each experiment 30+30 fields were captured, using a fluorescent Nikon Eclipse 80i microscope (40X lens) and a DS-2MBWC digital microscope camera. For each experiment, at least 150+150 β-tubulin$^+$ cells were sampled. Electronic files were imported in ImageJ. They were processed by NeuriteTracer® plug-in, according to authors' instructions (Pool et al., 2008), and NeuriteTracer® outputs, i.e. average neurite lengths per neuron calculated per each field, were collected. The experiment was repeated three times; data were analyzed as follows. Average neurite lengths per neuron calculated per each field were averaged per each experiment and each lentivirus. The results (± s.e.m.) were plotted against experiment numbers. Finally, the so-obtained 3+3 average frequencies were analyzed by t-test (1-tail, paired) and the p-value reported on the graph.

### 4.8 *In utero* electroporation

Electroporation was carried out to transfect VZ cells *in utero* with mammalian expression vectors as described previously [Gal et al, 2006, Saito et al, 2006; Walantus et al, 2007). Briefly, uterine horns of E12.5 pregnant dams were exposed by midline laparotomy after anesthetization with ketamine (200 µg/g bodyweight) and xylazine (40 µg/g bodyweight). 1.5 µl of a solution containing 3 µg of DNA plasmid, mixed with 0.02% fast-green dye in phosphate buffered saline (PBS), was injected in the telencephalic vesiscle using a sharp pulled micropipette (hole external diameter about 30 µm) through the uterine wall and the amniotic sac. Platinum tweezer-style

electrodes (7mm diameter) were placed outside the uterus over the telencephalon and four pulses of 40 mV were applied (each 50 ms long, interval between consecutive pulses 950 ms), by using a BTX ECM830 square wave pulse generator (Genetronics). Electroporation was performed in about half of the embryos found in each uterine horn, to avoid prolonged surgery time. The uterus was then replaced within the abdomen, the cavity was filled with warm sterile PBS, and the abdominal muscle and skin incisions were closed with silk sutures. Animals were left to recover in a warm clean cage. Harvesting of electroporated embryos was performed two days later, as described above.

**4.9 microRNAs *In situ* hybridization.**

Brains from E10.5 to E18.5 embryos and 4-or-15-days-old CD1 mice (Harlan lab), as well as brain from E14.5 embryos electroporated two days earlier were perfused with 4% paraformaldehyde (PFA) overnight. Afterwards, brains were immersed in 30% sucrose (wt/vol) and embedded in OCT mounting medium. *In situ* hybridization were carried out on 10 µm coronal brain slices using miRCURY 5' DIG labeled detection probes (LNA) for mmu-miR-124, mmu-miR-425 and mmu-miR-207 according to manufacturer's instructions (Exiqon®), as previously described (Kloosterman et al, 2006). To detect the Pri/Pre-miR-124(2) a miRCURY 5'-3' DIG double labeled detection probes (LNA) against the loop of the Pre-mir-124(2) was manufactured *ad hoc* from Exiqon® (sequence: GACCTTGATTTAATGTCATACAAT- mouse chr3:17,695,699-17,695,722) and *In situ* hybridization was carried out according to manufacturer's instructions (Exiqon®).

**4.10 Tissues Immunofluorescence.**

Immunofluorescence analyses were performed as previously described (Muzio and Mallamaci 2005). Briefly, frozen sections were boiled in 10 mM sodium citrate, pH 6.0, and blocked in 10% fetal bovine serum (FBS) and 0.1% Triton X-100 for 1 hr at room temperature. Incubation with primary antibodies was performed at 4ºC overnight. In the case of BrdU detection, epitopes were made accessible by HCl treatment, as previously described (. Secondary antibodies were applied to sections for 2 hr at room temperature. The following primary antibodies were used: anti-β-tubulin mouse monoclonal (clone Tuj1, Covance, 1:300), anti-Egfp chicken polyclonal (AbCam, 1:600), anti Phosphohistone-H3 rabbit polyclonal (Chemicon Upstate, 1:400), anti-Tbr1 rabbit polyclonal (a gift from R. Hevner, Seattle, USA, 1:2000), anti-Tbr2 rabbit polyclonal (AbCam, 1:600), anti-active_caspase3 rabbit polyclonal (Pharmige, 1:300), anti-Pax6 rabbit polyclonal (AbCam, 1:500), anti-β1-integrin rat monoclonal (clone VLA, Chemicon, 1:500), anti-BrdU

mouse monoclonal (clone B44, Becton Dickinson, 1:50). Secondary antibodies were conjugates of Alexa Fluor 488 and Alexa Fluor 594 (Invitrogen, 1:500). DAPI (4', 6'- diamidino-2-phenylindole) was used as nuclear counterstaining. Finally, slices were washed and mounted in Fluorescent Vectashield™ Mounting Medium. Immunofluorescence analyses on *in situ* hybridized coronal brain slices was performed as described above, after washing the LNA-hybridized sections for 1 hour in PBS.

### 4.11 Acquisition, processing and statistical analysis of in vivo immunoprofiling data.

*In situ* hybridized sections with or without immunofluorescence analysis were imaged using a fluorescent Nikon Eclipse 80i microscope and a DS-2MBWC digital microscope camera. Such images were processed by Adobe Photoshop CS3 software.

Per each marker subject of analysis, cell counting was performed on at least three different electroporated embryos, for both pPri-miR-124(2) and pPri-miR-155 constructs ($N \geq 3,3$); in turn, three sections from each electroporated embryo, 100 mm spaced along the rostro-caudal axis, were inspected. In total, at least 400 $EmGFP^+$ per each embryo were scored for double labeling, paying special attention to compare embryonic tissue electroporated at similar rostro-caudal and medial-lateral levels. Sections were photographed using a TCS SP2 Leica confocal microscope, generally collected as 5.0 µm-thick Z-stacks of 1024*1024 pixel images. Images were then imported into Photoshop CS3, where all cell countings were performed on coded samples, so that the experimenter was blind to the condition. Results were imported into Excel 2008, percentages of labeled cells were calculated for each brain and data relative to all brains electroporated with the same construct were averaged. Results were expressed as mean value ± standard error of the mean and were tested for statistical significance by One Way-ANOVA. Results were shown as normalized against controls.

# 5. List of abbreviations

**ANR,** anterior neural ridge
**CNS**, central nervous system
**CP**, cortical plate
**FCS**, fetal calf serum
**IZ,** intermediate zone
**IPCs**, intermediate precursor cells
**LGE,** lateral ganglionic eminence
**LncRNA,** long non coding RNA
**MAZ**, multipolar accumulation zone
**MGE,** medial ganglionic eminence
**MZ**, marginal zone
**ncRNA**, non coding RNA
**NEPs,** neuroepitelial cells
**NSC**, neural stem cell
**PI**, post infection
**PNS,** peripheral nervous system
**PP,** preplate
**RGCs,** radial glia cells
**SncRNA,** short non coding RNA
**SNPs**, short neural precursors
**SP**, subplate
**SVZ**, subventricular zone
**TCA,** thalamocortical axons
**TF**, transitional field
**TFs,** transcription factors
**VZ**, ventricular zone

# 6. References


Aaku-Saraste E, Hellwig A, Huttner WB. Loss of occludin and functional tight junctions, but not ZO-1, during neural tube closure-remodeling of the neuroepithelium prior to neurogenesis. Dev Biol. 1996 180(2):664-679

Aaku-Saraste, E, Oback, B., Hellwig, A. & Huttner, W. B. Neuroepithelial cells downregulate their plasma membrane polarity prior to neural tube closure and neurogenesis. Mech Dev. 1997; 69(1-2): 71-81

Adenot, X., Elmayan, T., Lauressergues, D., Boutet, S., Bouche, N., Gasciolli, V. and Vaucheret, H. DRB4-dependent TAS3 trans-acting siRNAs control leaf morphology through AGO7. 2006 Curr. Biol. 16, 927-932.

Amaral PP, Mattick JS. Noncoding RNA in development. Mamm Genome. 2008; (7-8):454-492.

Aravin, A., Gaidatzis, D., Pfeffer, S., Lagos-Quintana, M., Landgraf, P., Iovino, N., Morris, P., Brownstein, M. J., Kuramochi-Miyagawa, S., Nakano, T. et al. A novel class of small RNAs bind to MILI protein in mouse testes. 2006 Nature 442, 203-207.

Baehrecke EH. How death shapes life during development. Nat Rev Mol Cell Biol. 2002 (10):779-787

Baek D, Villén J, Shin C, Camargo FD, Gygi SP, Bartel DP. The impact of microRNAs on protein output. (2008) Nature 455, 64–71.

Ballas N, Grunseich C, Lu DD, Speh JC, Mandel G. REST and its corepressors mediate plasticity of neuronal gene chromatin throughout neurogenesis. Cell (2005);121(4):645-57

Bani-Yaghoub M, Tremblay RG, Lei JX, Zhang D, Zurakowski B, Sandhu JK, Smith B, Ribecco-Lutkiewicz M, Kennedy J, Walker PR, Sikorska M. Role of Sox2 in the development of the mouse neocortex. Dev Biol. 2006 1;295(1):52-66

Bartel DP. MicroRNAs: Genomics, Biogenesis, Mechanisms, and Function. 2004 Cell (116); 281-297

Bayer, S. A. and Altman, J. Neocortical Development (Raven, New York, 1991).

Berezikov E, Chung WJ, Willis J, Cuppen E, Lai EC. Mammalian mirtron genes. Mol Cell. 2007 28(2):328-336

Bernstein E, Kim SY, Carmell MA, Murchison EP, Alcorn H, Li MZ, Mills AA, Elledge SJ, Anderson KV, Hannon GJ. Dicer is essential for mouse development. 2003 Nat Genet. 2003 (3):215-217

Bertrand N, Castro DS, Guillemot F. Proneural genes and the specification of neural cell types. Nat Rev Neurosci. 2002 (7):517-530.

Betel, D., Sheridan, R., Marks, D. and Sander, C. Computational analysis of mouse piRNA sequence and biogenesis. 2007 PLoS Comp. Biol. 3, e222.

Bhattacharyya SN, Habermacher R, Martine U, Closs EI, Filipowicz W. Relief of microRNA-mediated translational repression in human cells subjected to stress. 2006 Cell 125(6):1111-24

Bielle F, Griveau A, Narboux-Nême N, Vigneau S, Sigrist M, Arber S, Wassef M, Pierani A. Multiple origins of Cajal-Retzius cells at the borders of the developing pallium. Nat Neurosci. 2005 8(8):1002-1012.

Bishop KM, Goudreau G, and O'Leary D. Regulation of area identity in the mammalian neocortex by Emx2 and Pax6. Science 2000; 288:344–349

Bohnsack MT, Czaplinski K, Gorlich D. Exportin 5 is a RanGTP-dependent dsRNA-binding protein that mediates nuclear export of pre-miRNAs. RNA. 2004 (2):185-191

Borchert GM, Lanier W, Davidson BL. RNA polymerase III transcribes human microRNAs. Nat Struct Mol Biol. 2006 (12):1097-101

Borsani, O., Zhu, J., Verslues, P. E., Sunkar, R. and Zhu, J. K. Endogenous siRNAs derived from a pair of natural cis-antisense transcripts regulate salt tolerance in Arabidopsis. 2005 Cell 123, 1279-1291.

Britten RJ, Davidson EH. Gene regulation for higher cells: a theory. Science. 1969 (891):349-357

Brockdorff N, Ashworth A, Kay GF, McCabe VM, Norris DP, Cooper PJ, Swift S, Rastan S. The product of the mouse Xist gene is a 15 kb inactive X-specific transcript containing no conserved ORF and located in the nucleus. Cell. (1992) 71(3):515-526.

Cao X, Pfaff SL, Gage FH. A functional study of miR-124 in the developing neural tube. Genes Dev (2007) 21,(5):531-536

Carninci P, Kasukawa T, Katayama S, Gough J, Frith MC et al. (2005). The transcriptional landscape of the mammalian genome. Science 309:1559–1563

Carthew RW, Sontheimer EJ. Origins and Mechanisms of miRNAs and siRNAs (2009). Cell. 2009 136(4):642-655

Caviness VS, Bhide PG, Nowakowski RS. Histogenetic processes leading to the laminated neocortex: migration is only a part of the story. Dev Neurosci. 2008 (1-3):82-95

Chang, S., Johnston, R. J. Jr, Frokjaer-Jensen, C., Lockery, S. & Hobert, O. MicroRNAs act sequentially and asymmetrically to control chemosensory laterality in the nematode. (2004) Nature 430, 785–789

Cheng LC, Pastrana E, Tavazoie M, Doetsch F. miR-124 regulates adult neurogenesis in the subventricular zone stem cell niche. Nat Neuroscience (2009) 12(4):399-408.

Cherubini E, Conti F. Generating diversity at GABAergic synapses. Trends Neurosci. 2001 24(3):155-162

Conaco C, Otto S, Han JJ, Mandel G. Reciprocal actions of REST and a microRNA promote neuronal identity. Proc Natl Acad Sci (2006) 103(7):2422-2427

Cubelos B, Sebastián-Serrano A, Kim S, Moreno-Ortiz C, Redondo JM, Walsh CA, Nieto M. Cux-2 controls the proliferation of neuronal intermediate precursors of the cortical subventricular zone. Cereb Cortex. 2008 (8):1758-1770.

Cullen BR, Viruses and microRNAs, Nature Genetics 38, (2006) S25 - S30

Darr H, Benvenisty N. Genetic analysis of the role of the reprogramming gene LIN-28 in human embryonic stem cells. Stem Cells. 2009 (2):352-362.

Davis BN, Hilyard AC, Lagna G, Hata A. SMAD proteins control DROSHA-mediated microRNA maturation. Nature. 2008 45-(7200):56-61

De Pietri Tonelli D, Calegari F, Fei JF, Nomura T, Osumi N, Heisenberg CP, Huttner WB: Single-cell detection of microRNAs in developing vertebrate embryos after acute administration of a dual-fluorescence reporter/sensor plasmid. Biotechniques 2006, 41(6):727-732.

De Pietri Tonelli D, Pulvers JN, Haffner C, Murchison EP, Hannon GJ, Huttner WB. miRNAs are essential for survival and differentiation of newborn neurons but not for expansion of neural progenitors during early neurogenesis in the mouse embryonic neocortex. Development (2008) 135(23):3911-21

Dehay C, Kennedy H. Cell-cycle control and cortical development. Nat Rev Neurosci. 2007 8(6):438-450

Deo M, Yu JY, Chung KH, Tippens M, Turner DL: Detection of mammalian microRNA expression by in situ hybridization with RNA oligonucleotides. Dev Dyn 2007, 235(9):2538-2548

Diederichs S, Haber DA. Dual role for argonautes in microRNA processing and posttranscriptional regulation of microRNA expression. (2007) Cell. 2007 (6):1097-1108.

Dorsett, Y. and Tuschl, T. siRNAs: applications in functional genomics and potential as therapeutics. (2004). Nat. Rev. Drug Discov. 318-329.

Edwards MA, Yamamoto M, Caviness VS. Organization of radial glia and related cells in the developing murine CNS. An analysis based upon a new monoclonal antibody marker. Neuroscience 1990 36:121–144

Elbashir, S. M., Lendeckel, W. and Tuschl, T. RNA interference is mediated by 21- and 22-nucleotide RNAs. 2001 Genes Dev. 15, 188-200.

Elbashir, S. M., Harborth, J., Lendeckel, W., Yalcin, A., Weber, K. and Tuschl, T. Duplexes of 21-nucleotide RNAs mediate RNA interference in cultured mammalian cells. (2001b) Nature 411, 494-498.

Englund C, Fink A, Lau C, Pham D, Daza RA, Bulfone A, Kowalczyk T, Hevner RF. Pax6, Tbr2, and Tbr1 are expressed sequentially by radial glia, intermediate progenitor cells, and postmitotic neurons in developing neocortex. J Neurosci. 2005 25(1):247-251

Farazi TA, Juranek SA, Tuschl T. The growing catalog of small RNAs and their association with distinct Argonaute/Piwi family members. Development. 2008 135(7):1201-1214.

Feng L, Hatten ME, Heintz N. Brain lipid-binding protein (BLBP): a novel signaling system in the developing mammalian CNS. Neuron. 1994 12(4):895-908

Feng Y, Walsh CA. Protein-protein interactions, cytoskeletal regulation and neuronal migration. Nat Rev Neurosci. 2001 2(6):408-416

Flynt AS, Lai EC. Biological principles of microRNA-mediated regulation: shared themes amid diversity. 2008 Nat Rev Genet. (11):831-42.

Follenzi A, Naldini L: Generation of HIV-1 derived lentiviral vectors. Methods Enzymol 2002, 346:454-465.

Forman, J. J., Legesse-Miller, A. & Coller, H. A. A search for conserved sequences in coding regions reveals that the let-7 microRNA targets Dicer within its coding sequence. (2008) Proc. Natl Acad. Sci. 105, 14879–14884.

Frantz GD, McConnell SK. Restriction of late cerebral cortical progenitors to an upper-layer fate. Neuron. 1996 (1):55-61.

Frederiksen K, McKay RD. Proliferation and differentiation of rat neuroepithelial precursor cells in vivo. J Neurosci. 1988 (4):1144-1151.

Fukuda T, Yamagata K, Fujiyama S, Matsumoto T et al. DEAD-box RNA helicase subunits of the Drosha complex are required for processing of rRNA and a subset of microRNAs. Nat Cell Biol. 2007 (5):604-611.

Gal JS, Morozov YM, Ayoub AE, Chatterjee M, Rakic P, Haydar TF. Molecular and morphological heterogeneity of neural precursors in the mouse neocortical proliferative zones. J Neurosci. 2006 26(3):1045-1056

Gilbert, S.F. 2003 7th edition. Developmental Biology. Sinauer Associates, Inc., Sunderland, MA.

Giraldez, A. J. et al. Zebrafish MiR-430 promotes deadenylation and clearance of maternal mRNAs. 2006 Science 312, 75–79.

Götz M, Huttner WB. The cell biology of neurogenesis. Nat Rev Mol Cell Biol. 2005 6(10):777-788

Graus-Porta D, Blaess S, Senften M, Littlewood-Evans A, Damsky C, Huang Z, Orban P, Klein R, Schittny JC, Müller U: Beta1-class integrins regulate the development of laminae and folia in the cerebral and cerebellar cortex. Neuron 2001, 31(3):367-379.

Gregory RI, Yan KP, Amuthan G, Chendrimada T, Doratotaj B, Cooch N, Shiekhattar R. The Microprocessor complex mediates the genesis of microRNAs. Nature. 2004; 432(7014):235-240.

Griffiths-Jones S, Grocock RJ, van Dongen S, Bateman A, Enright AJ: miRBase: microRNA sequences, targets and gene nomenclature. Nucleic Acids Res, 34:140-144 (2006).

Grimson A, Farh KK, Johnston WK, Garrett-Engele P, Lim LP, Bartel DP: MicroRNA targeting specificity in mammals: determinants beyond seed pairing. Mol Cell 2006, 27(1):91-105

Gritti A, Parati EA, Cova L, Frolichsthal P, Galli R, Wanke E, Faravelli L, Morassutti DJ, Roisen F, Nickel DD, Vescovi AL: Multipotential stem cells from the adult mouse brain proliferate and self-renew in response to basic fibroblast growth factor. J Neurosci 1996, 16(3):1091-1100

Guillemot F. Cellular and molecular control of neurogenesis in the mammalian telencephalon. Curr Opin Cell Biol. 2005 17(6):639-647

Haubensak W, Attardo A, Denk W, Huttner WB Neurons arise in the basal neuroepithelium of the early mammalian telencephalon: a major site of neurogenesis. Proc Natl Acad Sci U S A. 2004 (9):3196-3201

Hartfuss E, Galli R, Heins N, Götz M. Characterization of CNS precursor subtypes and radial glia. Dev Biol. 2001; 229(1):15-30

Hashimoto-Torii K, Torii M, Sarkisian MR, Bartley CM, Shen J, Radtke F, Gridley T, Sestan N, Rakic P. Interaction between Reelin and Notch signaling regulates neuronal migration in the cerebral cortex. Neuron. 2008 60(2):273-284

Heins N, Malatesta P, Cecconi F, Nakafuku M, Tucker KL, Hack MA, Chapouton P, Barde YA, Götz M. Glial cells generate neurons: the role of the transcription factor Pax6. Nat Neurosci. 2002 (4):308-315.

Hébert JM, Fishell G. The genetics of early telencephalon patterning: some assembly required. Nat Rev Neurosci. 2008 (9):678-685.

Hirota K, Miyoshi T, Kugou K, Hoffman CS, Shibata T, Ohta K. Stepwise chromatin remodelling by a cascade of transcription initiation of non-coding RNAs. Nature. 2008 6 (7218):130-134.

Huang Z. Molecular regulation of neuronal migration during neocortical development. Mol Cell Neurosci. 2009; 42(1):11-22

Hwang HW, Wentzel EA, Mendell JT. A hexanucleotide element directs microRNA nuclear import. Science. 2007 (5808):97-100

Hwang HW, Wentzel EA, Mendell JT: Cell-cell contact globally activates microRNA biogenesis. Proc Natl Acad Sci USA 2009, 106(17):7016-7021.

Kanellopoulou C, Muljo SA, Kung AL, Ganesan S, Drapkin R, Jenuwein T, Livingston DM, Rajewsky N: Dicer-deficient mouse embryonic stem cells are defective in differentiation and centromeric silencing. Genes Dev 2005, 19(4):489-501.

Karres, J. S., Hilgers, V., Carrera, I., Treisman, J. Cohen, S. M. The conserved microRNA miR-8 tunes atrophin levels to prevent neurodegeneration in Drosophila. (2007) Cell 131, 136–145

Kawahara Y, Zinshteyn B, Chendrimada TP, Shiekhattar R, Nishikura K. RNA editing of the microRNA-151 precursor blocks cleavage by the Dicer-TRBP complex. EMBO Rep. 2007 (8):763-769

Kawahara Y, Zinshteyn B, Sethupathy P, Iizasa H, Hatzigeorgiou AG, Nishikura K. Redirection of silencing targets by adenosine-to-inosine editing of miRNAs. 2007 Science. 315(5815):1137-1140

Kedde M, Strasser MJ, Boldajipour B et al. RNA-binding protein Dnd1 inhibits microRNA access to target mRNA. Cell. 2007 131(7):1273-1286.

Kertesz, M., Iovino, N., Unnerstall, U., Gaul, U., Segal, E. The role of site accessibility in microRNA target recognition. (2007) Nature Genet. 39, 1278–1284.

Kim, D. H., Saetrom, P., Snove, O. Jr & Rossi, J. J. MicroRNA-directed transcriptional gene silencing in mammalian cells. (2008) Proc. Natl Acad. Sci. 105, 16230–16235.

Kim J, Inoue K, Ishii J, Vanti WB, Voronov SV, Murchison E, Hannon G, Abeliovich A. A MicroRNA feedback circuit in midbrain dopamine neurons. Science. 2007 317(5842):1220-1224

Kim VN. MicroRNA biogenesis: coordinated cropping and dicing. Nat Rev Mol Cell Biol. 2005 (5):376-385.

Kim YK, Kim VN. Processing of intronic microRNAs. EMBO J. 2007 26(3):775-783

Kloosterman WP, Wienholds E, de Bruijn E, Kauppinen S, Plasterk RH: In situ detection of miRNAs in animal embryos using LNA-modified oligonucleotide probes. Nat Methods 2006, 3(1):27-29.

Krek A, Grün D, Poy MN, Wolf R, Rosenberg L, Epstein EJ, MacMenamin P, Piedade I, Gunsalus KC, Stoffel M, Rajewsky N: Combinatorial microRNA target predictions. Nat Genet 2005, 37(5):495-500.

Krichevsky AM, King KS, Donahue CP, Khrapko K, Kosik KS. A microRNA array reveals extensive regulation of microRNAs during brain development. RNA. 9(10):1274-1281 (2003)

Krichevsky AM, Sonntag KC, Isacson O, Kosik KS. Specific microRNAs modulate embryonic stem cell-derived neurogenesis. Stem Cells (2006) (4):857-864

Kosodo Y, Huttner WB. Basal process and cell divisions of neural progenitors in the developing brain. Dev Growth Differ. 2009 51(3):251-261

Kosodo Y, Roper K, Haubensak W, Marzesco AM, Corbeil D, Huttner WB. Asymmetric distribution of the apical plasma membrane during neurogenic divisions of mammalian neuroepithelial cells. EMBO J. 2004 23(11):2314-2324

Kowalczyk T, Pontious A, Englund C, Daza RA, Bedogni F, Hodge R, Attardo A, Bell C, Huttner WB, Hevner RF. Intermediate Neuronal Progenitors (Basal Progenitors) Produce Pyramidal-Projection Neurons for All Layers of Cerebral Cortex. Cereb Cortex. 2009

Lagos-Quintana M, Rauhut R, Yalcin A, Meyer J, Lendeckel W, Tuschl T: Identification of tissue-specific microRNAs from mouse. Curr Biol, 12(9):735-739 (2002).

Lagos-Quintana M, Rauhut R, Meyer J, Borkhardt A, Tuschl T: New microRNAs from mouse and human. RNA 2003, 9:175-179.

Lai, E. C. microRNAs are complementary to 3′ UTR sequence motifs that mediate negative posttranscriptional regulation. Nature Genet. 30, 363–364 (2002)

Landgraf P, Rusu M et al.: A mammalian microRNA expression atlas based on small RNA library sequencing. Cell 2007, 129:1401-1414.

Lau P, Verrier JD, Nielsen JA, Johnson KR, Notterpek L, Hudson LD. Identification of dynamically regulated microRNA and mRNA networks in developing oligodendrocytes. J Neurosci. (2008) 28(45):11720-11730

Lee, R. C., Feinbaum, R. L. & Ambros, V. The C. elegans heterochronic gene lin-4 encodes small RNAs with antisense complementarity to lin-14. (1993) Cell 75, 843–854

Lee Y, Kim M, Han J, Yeom KH, Lee S, Baek SH, Kim VN. MicroRNA genes are transcribed by RNA polymerase II. EMBO J. 2004 23(20):4051-60

Li X, Carthew RW. A microRNA mediates EGF receptor signaling and promotes photoreceptor differentiation in the Drosophila eye. Cell. 2005 123(7):1267-1277

Li, J., Yang, Z., Yu, B., Liu, J. & Chen, X. Methylation protects miRNAs and siRNAs from a 3´-end uridylation activity in Arabidopsis. (2005) Curr. Biol. 15, 1501–1507

Lytle, J. R., Yario, T. A. & Steitz, J. A. Target mRNAs are repressed as efficiently by microRNA-binding sites in the 5′ UTR as in the 3′ UTR. (2007) Proc. Natl Acad. Sci. 104, 9667–9672.

Liu, J., Carmell, M. A., Rivas, F. V., Marsden, C. G., Thomson, J. M., Song, J. J., Hammond, S. M., Joshua-Tor, L. and Hannon, G. J. Argonaute2 is the catalytic engine of mammalian RNAi. 2004 Science 305, 1437-1441.

Lim, L. P. et al. Microarray analysis shows that some microRNAs downregulate large numbers of target mRNAs. 2005 Nature 433, 769–773.

Liu A, Niswander LA. Bone morphogenetic protein signalling and vertebrate nervous system development. Nat Rev Neurosci. 2005 Dec; 6(12):945-954.

LoTurco JJ, Bai J. The multipolar stage and disruptions in neuronal migration. Trends Neurosci. 2006 29(7):407-413

Luciano DJ, Mirsky H, Vendetti NJ, Maas S. RNA editing of a miRNA precursor. RNA. 2004 (8):1174-1177

Lund E, Güttinger S, Calado A, Dahlberg JE, Kutay U. Nuclear export of microRNA precursors. Science. 2004 303(5654):95-98

Lujambio A, Calin GA, Villanueva A, Ropero S, Sánchez-Céspedes M, Blanco D, Montuenga LM, Rossi S, Nicoloso MS, Faller WJ, Gallagher WM, Eccles SA, Croce CM, Esteller M. A microRNA DNA methylation signature for human cancer metastasis. Proc Natl Acad Sci U S A. 2008 105(36):13556-13561

MacRae IJ, Ma E, Zhou M, Robinson CV, Doudna JA. In vitro reconstitution of the human RISC-loading complex. Proc Natl Acad Sci U S A. 2008 105(2):512-517

Makeyev EV, Zhang J, Carrasco MA, Maniatis T. The MicroRNA miR-124 promotes neuronal differentiation by triggering brain-specific alternative pre-mRNA splicing. Mol Cell. 2007 27(3):435-448

Malatesta P, Hartfuss E, Götz M. Isolation of radial glial cells by fluorescent-activated cell sorting reveals a neuronal lineage. Development. 2000; 27(24):5253-5263.

Malatesta P, Hack MA, Hartfuss E, Kettenmann H, Klinkert W, Kirchhoff F, Götz M. Neuronal or glial progeny: regional differences in radial glia fate. Neuron. 2003 37(5):751-764

Malatesta P, Apolloni I, Calzolari F. Radial glia and neural stem cells. Cell Tissue Res. 2008 331(1):165-178

Mallamaci A, Muzio L, Chan CH, Parnavelas J, Boncinelli E. Area identity shifts in the early cerebral cortex of Emx2-/- mutant mice. Nat Neurosci. 2000 3(7):679-686.

Mallamaci A, Stoykova A. Gene networks controlling early cerebral cortex arealization. Eur J Neurosci. 2006 Feb; (4):847-856.

Marín O, Rubenstein JL. A long, remarkable journey: tangential migration in the telencephalon. Nat Rev Neurosci. 2001 2(11):780-790.

Marín O, Rubenstein JL. Cell migration in the forebrain. Annu Rev Neurosci. 2003;26:441-483

Martens JA, Wu PY, Winston F. Regulation of an intergenic transcript controls adjacent gene transcription in Saccharomyces cerevisiae. Genes Dev. 2005 15;19(22):2695-2704

Mattick JS. A new paradigm for developmental biology. 2007 J Exp Biol 210:1526–1547

McConnell SK, Kaznowski CE. Cell cycle dependence of laminar determination in developing neocortex. Science. 1991 (11)-282-285

Michlewski G, Guil S, Semple CA, Cáceres JF. Posttranscriptional regulation of miRNAs harboring conserved terminal loops. Mol Cell. 2008 32(3):383-393

Molyneaux BJ, Arlotta P, Menezes JR, Macklis JD. Neuronal subtype specification in the cerebral cortex. Nature Review Neuroscience. 2007 Jun;8(6):427-437.

Monuki ES, Walsh CA. Mechanisms of cerebral cortical patterning in mice and humans. Nat Neurosci. 2001 Nov; 4(1199-1206)

Morlando M, Ballarino M, Gromak N, Pagano F, Bozzoni I, Proudfoot NJ. Primary microRNA transcripts are processed co-transcriptionally. Nat Struct Mol Biol. 2008 15(9):902-909

Muzio L, DiBenedetto B, Stoykova A, Boncinelli E, Gruss P, Mallamaci A. Conversion of cerebral cortex into basal ganglia in Emx2(-/-) Pax6 (Sey/Sey) double-mutant mice. Nat Neurosci. 2002 Aug;5(8):737-745.

Muzio L, Mallamaci A: Foxg1 confines Cajal-Retzius Neuronogenesis and Hippocampal Morphogenesis to the Dorsomedial Pallium. *J Neurosci* 2005, 25(17):4435-41.

Nadarajah, B., and J.G. Parnavelas. Modes of neuronal migration in the developing cerebral cortex. Nat Rev Neurosci. 2002 3:423-432.

Noctor SC, Martínez-Cerdeño V, Ivic L, Kriegstein AR. Cortical neurons arise in symmetric and asymmetric division zones and migrate through specific phases. Nat Neurosci. 2004 (2):136-144.

Obernosterer, G., Leuschner, P. J., Alenius, M. & Martinez, J. Post-transcriptional regulation of microRNA expression. (2006) RNA 1161–1167.

Ochiai W, Minobe S, Ogawa M, Miyata T. Transformation of pin-like ventricular zone cells into cortical neurons. Neurosci Res. 2007; 57(2):326-329.

Ochiai W, Nakatani S, Takahara T, Kainuma M, Masaoka M, Minobe S, Namihira M, Nakashima K, Sakakibara A, Ogawa M and Miyata T: Periventricular notch activation and asymmetric Ngn2 and Tbr2 expression in pair-generated neocortical daughter cells. Mol Cell Neurosci 2009, 40:225-233.

O'Donnell, K. A. and Boeke, J. D.. Mighty Piwis defend the germline against genome intruders. 2007 Cell 129, 37-44.

O'Donnell KA, Wentzel EA, Zeller KI, Dang CV, Mendell JT. c-Myc-regulated microRNAs modulate E2F1 expression. Nature. 2005 Jun 435(7043):839-843

O'Leary DD, Chou SJ, Sahara S. Area patterning of the mammalian cortex. Neuron. 2007 56(2):252-269.

O'Leary DD, Nakagawa Y. Patterning centers, regulatory genes and extrinsic mechanisms controlling arealization of the neocortex. Curr Opin Neurobiol. 2002 12(1):14-25

Place, R. F., Li, L. C., Pookot, D., Noonan, E. J. & Dahiya, R. MicroRNA-373 induces expression of genes with complementary promoter sequences. (2008) Proc. Natl Acad. Sci. 105, 1608–1613.

Ponting CP, Oliver PL, Reik W. Evolution and functions of long noncoding RNAs. 2009 Cell 20;136(4):629-641

Pontious A, Kowalczyk T, Englund C, Hevner RF. Role of intermediate progenitor cells in cerebral cortex development. Dev Neurosci. 2008; (30) 24-32.

Pool M, Thiemann J, Bar-Or A, Fournier AE. NeuriteTracer: a novel ImageJ plugin for automated quantification of neurite outgrowth. J Neurosci Methods. 2008 168(1):134-139

Rallu M, Corbin JG, Fishell G. Parsing the prosencephalon. Nat Rev Neurosci. 2002 Dec (12):943-951

Rakic P, Ayoub AE, Breunig JJ, Dominguez MH., Decision by division: making cortical maps. Trends Neurosci. 2009 32:291-301.

Rakic P., A small step for the cell, a giant leap for mankind: a hypothesis of neocortical expansion during evolution. Trends Neurosci. 1995 (9):383-388.

Rakic P. Developmental and evolutionary adaptations of cortical radial glia. Cereb Cortex. 2003 (6):541-549.

Rash BG, Grove EA. Area and layer patterning in the developing cerebral cortex. Curr Opin Neurobiol. 2006; 16(1):25-34.

Ross, S.E., Greenberg M.E., and Stiles. C.D. Basic helix-loop-helix factors in cortical development. Neuron. 2003. 39:13-25.

Ruby JG, Jan CH, Bartel DP. Intronic microRNA precursors that bypass Drosha processing. Nature 2007 448(7149):83-86

Rybak, A. et al. A feedback loop comprising lin-28 and let-7 controls pre-let-7 maturation during neural stem-cell commitment. (2008) Nature Cell Biol. 10, 987–993.

Salzman, D. W., Shubert-Coleman, J. & Furneaux, H. P68 RNA helicase unwinds the human let-7 microRNA precursor duplex and is required for let-7-directed silencing of gene expression. (2007) J. Biol. Chem. 282, 32773–32779

Saito, T: In vivo electroporation in the embryonic mouse central nervous system. Nat Protocols 2006, 1:1552–1558.

Sastry L, Johnson T, Hobson MJ, Smucker B, Cornetta K: Titering lentiviral vectors: comparison of DNA, RNA and marker expression methods. Gene Ther 2006, 9(17):1155-1162.

Schratt GM, Tuebing F, Nigh EA, Kane CG, Sabatini ME, Kiebler M, Greenberg ME. brain-specific microRNA regulates dendritic spine development. Nature. 2006 439(7074):283-289

Sessa A, Mao CA, Hadjantonakis AK, Klein WH, Broccoli V. Tbr2 directs conversion of radial glia into basal precursors and guides neuronal amplification by indirect neurogenesis in the developing neocortex. Neuron. 2008 Oct 9;60(1):56-69

Selbach M, Schwanhäusser B, Thierfelder N, Fang Z, Khanin R, Rajewsky N. Widespread changes in protein synthesis induced by microRNAs. Nature 2008 455(7209):58-63.

Shibata T, Yamada K, Watanabe M, Ikenaka K, Wada K, Tanaka K, Inoue Y. Glutamate transporter GLAST is expressed in the radial glia-astrocyte lineage of developing mouse spinal cord. J Neurosci. 1997 17(23):9212-9219.

Shibata M, Kurokawa D, Nakao H, Ohmura T, Aizawa S. MicroRNA-9 modulates Cajal-Retzius cell differentiation by suppressing Foxg1 expression in mouse medial pallium. J Neurosci. (2008) 8;28

Sleutels F, Zwart R, Barlow DP. The non-coding Air RNA is required for silencing autosomal imprinted genes. Nature (2002) 14 (6873):810-813

Smirnova L, Gräfe A, Seiler A, Schumacher S, Nitsch R, Wulczyn FG. Regulation of miRNA expression during neural cell specification. Eur J Neuroscience (2005) 21(6):1469-1477

Stefani G, Slack FJ. Small non-coding RNAs in animal development. Nat Rev Mol Cell Biol. 2008 (3):219-230.

Tabata H, Kanatani S, Nakajima K: Differences of Migratory Behavior between Direct Progeny of Apical Progenitors and Basal Progenitors in the Developing Cerebral Cortex. Cereb Cortex 2009, doi:10.1093/cercor/bhn260

Taft RJ, Pheasant M, Mattick JS. The relationship between non-protein-coding DNA and eukaryotic complexity. Bioessays. 2007 (3):288-99

Tarabykin V, Stoykova A, Usman N, Gruss P. Cortical upper layer neurons derive from the subventricular zone as indicated by Svet1 gene expression. Development. 2001; (11):1983-1993

Tissir F, Goffinet M. Reelin and brain development. Nat Rev Neurosci. 2003; 4(6):496-505

Thomson JM, Parker J, Perou CM, Hammond SM. A custom microarray platform for analysis of microRNA gene expression. Nat Methods. (2004) 1(1):47-53

Thomson JM, Newman M, Parker JS, Morin-Kensicki EM, Wright T, Hammond SM: Extensive post-transcriptional regulation of microRNAs and its implications for cancer. Genes Dev 2006, 20(16):2202-2207.

Vagin, V. V., Sigova, A., Li, C., Seitz, H., Gvozdev, V. and Zamore, P. D. A distinct small RNA pathway silences selfish genetic elements in the germline. (2006) Science 313, 320-324.

Vasudevan S, Steitz JA. AU-rich-element-mediated upregulation of translation by FXR1 and Argonaute 2. (a) (2007) Cell 128(6):1105-1118

Vasudevan S, Tong Y, Steitz JA. Switching from repression to activation: microRNAs can up-regulate translation. (b) (2007) Science 318(5858):1877-1878. Vazquez, F. Arabidopsis endogenous small RNAs: highways and byways. 2006 Trends Plant Sci. 11, 460-468.

Visvanathan J, Lee S, Lee B, Lee JW, Lee SK. The microRNA miR-124 antagonizes the anti-neural REST/SCP1 pathway during embryonic CNS development. Genes Dev (2007) 21,(7):744-749

Viswanathan SR, Daley GQ, Gregory RI. Selective blockade of microRNA processing by Lin28. Science. 2008 (5872):97-100.

Vives V, Alonso G, Solal AC, Joubert D, Legraverend C. Visualization of S100B-positive neurons and glia in the central nervous system of EGFP transgenic mice. J Comp Neurol. 2003; 457(4):404-419

Walantus W, Castaneda D, Elias L, Kriegstein A: In utero intraventricular injection and electroporation of E15 mouse embryos. J Vis Exp 2007, 6:239.

Wang X, Arai S, Song X, Reichart D, Du K et al. Induced ncRNAs allosterically modify RNA-binding proteins in cis to inhibit transcription (2008) Nature 454:126–130

Watanabe, T., Takeda, A., Tsukiyama, T., Mise, K., Okuno, T., Sasaki, H., Minami, N. and Imai, H. Identification and characterization of two novel classes of small RNAs in the mouse germline: retrotransposon-derived siRNAs in oocytes and germline small RNAs in testes. 2006 Genes Dev. 20, 1732-1743.

Wienholds E, Kloosterman WP, Miska E, Alvarez-Saavedra E, Berezikov E, de Bruijn E, Horvitz HR, Kauppinen S, Plasterk RH. MicroRNA expression in zebrafish embryonic development. Science (2005) 309 (5732):310-311

Wilson SW, Rubenstein JL. Induction and dorsoventral patterning of the telencephalon. Neuron. 2000 Dec; (3):641-651.

Winter J, Jung S, Keller S, Gregory RI, Diederichs S. Many roads to maturity: microRNA biogenesis pathways and their regulation. Nat Cell Biol. 2009 (3):228-234

Wonders CP, Anderson SA. The origin and specification of cortical interneurons. Nat Rev Neurosci. 2006 (9):687-696

Wray GA. The evolutionary significance of cis-regulatory mutations. 2007 Nat Rev Genet 8:206–216

Wulczyn FG, Smirnova L, Rybak A, Brandt C, Kwidzinski E, Ninnemann O, Strehle M, Seiler A, Schumacher S, Nitsch R: Post-transcriptional regulation of the let-7 microRNA during neural cell specification. FASEB J 2007, 21(2):415-426.

Xu XL, Li Y, Wang F, Gao FB: The steady-state level of the nervous-system-specific microRNA-124a is regulated by dFMR1 in Drosophila. J Neurosci 2008, 28(46):11883-11889.

Yamazaki H, Sekiguchi M, Takamatsu M, Tanabe Y, Nakanishi S. Distinct ontogenic and regional expressions of newly identified Cajal-Retzius cell-specific genes during neocorticogenesis. Proc Natl Acad Sci 2004 101(40):14509-14

Yang W, Chendrimada TP, Wang Q, Higuchi M, Seeburg PH, Shiekhattar R, Nishikura K. Modulation of microRNA processing and expression through RNA editing by ADAR deaminases. 2006 Nat Struct Mol Biol. 13(1):13-21.

Yi R, Qin Y, Macara IG, Cullen BR. Exportin-5 mediates the nuclear export of pre-microRNAs and short hairpin RNAs. 2003 Genes Dev. 17(24):3011-3016

Yigit, E., Batista, P. J., Bei, Y., Pang, K. M., Chen, C. C., Tolia, N. H., Joshua- Tor, L., Mitani, S., Simard, M. J. and Mello, C. C. Analysis of the C. elegans Argonaute family reveals that distinct Argonautes act sequentially during RNAi. (2006) Cell 127, 747-757

Yoo AS, Staahl BT, Chen L, Crabtree GR. MicroRNA-mediated switching of chromatin-remodelling complexes in neural development. Nature (2009) 460(7255):642-646

Yoon K, Gaiano N. Notch signaling in the mammalian central nervous system: insights from mouse mutants. Nat Neurosci. 2005 8(6):709-715

Yu JY, Chung KH, Deo M, Thompson RC, Turner DL. MicroRNA miR-124 regulates neurite outgrowth during neuronal differentiation. Exp Cell Res. 2008 (14):2618-2633

Zhao Y, Samal E, Srivastava D: (2005). Serum response factor regulates a muscle-specific microRNA that targets Hand2 during cardiogenesis. Nature 2005, 436:181-182

Zhao, C., Guan, W., and Pleasure, S.J. A transgenic marker mouse line labels Cajal-Retzius cells from the cortical hem and thalamocortical axons. 2006 Brain Res. 1077, 48–53.

Zhao C, Sun G, Li S, Shi Y. A feedback regulatory loop involving microRNA-9 and nuclear receptor TLX in neural stem cell fate determination. Nat Struct Mol Biol. (2009) 16(4):365-371